

Smart Photochromic Materials Triggered with Visible Light

Anna-Lena Leistner^[a] and Zbigniew L. Pianowski^{*,[a, b]}

Molecular photoswitches reversibly convert the energy of light into a variety of structural changes at the molecular level. They can be integrated into smart materials with broad range of applicability. While most photochromic systems require UV light for activation, application of photoswitches operational entirely within the visible or NIR range of light brings considerable benefits, such as biocompatibility, better light penetration

through the material, propelling with sunlight, or a possibility to design dual systems that are mutually activated with UV or visible light frequencies for two distinct functions. In this Review, we discuss the most relevant classes of molecular photoswitches, and demonstrate a selection of photochromic polymers, gels, porous materials, surfaces, energy-storing materials and other systems triggered with visible light.

1. Introduction

Molecular photoswitches are molecules that reversibly interconvert between two forms, A and B, with distinct absorption spectra upon irradiation with light.^[1] This results in photochromism, defined as a light-induced reversible change of color.^[2] The interconversion usually relays on *E/Z* isomerizations^[3] or pericyclic reactions.^[4] The first mechanism typically results in distinct structural modifications, whereas the latter one often causes large changes in electronic properties and/or polarity. These effects render photoswitches useful for optical manipulation of various materials with high spatiotemporal precision, enabling a broad spectrum of applications. Photoswitches are classified as T- or P-types – with the return to the thermodynamically stable form A (“back-reaction”) occurring either thermally (T) or photochemically (P). Furthermore, we distinguish between the positive ($\lambda_{\text{max}}(\text{A}) < \lambda_{\text{max}}(\text{B})$) and negative ($\lambda_{\text{max}}(\text{A}) > \lambda_{\text{max}}(\text{B})$) photochromism.^[2,5]

Various aspects of the molecular photochromism can be discussed in details and have been recently reviewed, such as photoswitching in aqueous environment,^[6] applications in medicine,^[7] or in catalysis,^[8] reversible solid-to-liquid phototransitions,^[9] photochromism of materials,^[10] including photoresponsive porous,^[11] or soft materials,^[12] photochromic ligands in metal complexes,^[13] or photoswitchable peptides^[14] and saccharides.^[15]

Here we want to discuss a distinct facet and review the recent progress in the area of materials containing visible-light-activated molecular photoswitches. Specifically, we only demonstrate materials triggered with light frequencies above 400 nm.

Photoswitches are frequently used in the biological context^[16] and in photopharmacology.^[17] There, one of the major limiting factor is the highly energetic UV light required to isomerize the switches in at least one direction. Due to efficient absorption by biomolecules and scattering on cellular components, UV light cannot efficiently penetrate soft tissues or cells,^[18] and is disturbing *in vivo* analyses by its harmful effect on cellular processes.^[19] As a result, the scientific community working on organic photoswitches was highly motivated to invent optimized photochromic compounds addressable entirely with visible light.

In addition to broadening applicability in biological systems, we will also demonstrate the benefits of visible light switching in various classes of phototriggered materials, as exemplified by photoresponsive polymers, hydrogels, porous organic materials, surfaces, molecular platforms, and compounds intended for applications in solar thermal energy storage.

The important advantage is increased stability of the whole experimental setup. Shorter wavelengths (and, in particular, highly energetic UV light) are more damaging to the surroundings of the switch as compared to the longer wavelengths. This is exemplified by a visible-light-triggered (450/520 nm) catalytic system based on a hemithioindigo molecular motor, where the catalyst and the substrate are degraded or inactivated with light below 435 nm.^[20]

In this review, we have particularly focused on recent examples, and broad selection of the applied types of molecular photoswitches.

2. Visible-Light-Triggered Molecular Photoswitches

The main challenge in design of visible-light-triggered systems, including molecular switches,^[21] is the fact that nonradiative

[a] A.-L. Leistner, Dr. Z. L. Pianowski
Institut für Organische Chemie (IOC)
Karlsruher Institut für Technologie
Fritz-Haber-Weg 6, 76131 Karlsruhe, Germany
E-mail: pianowski@kit.edu
<https://www.ioc.kit.edu/pianowski/>

[b] Dr. Z. L. Pianowski
Institute of Biological and Chemical Systems – Functional Molecular Systems (IBCS-FMS)
Karlsruher Institut für Technologie
Hermann-von-Helmholtz-Platz 1, 76344 Eggenstein-Leopoldshafen, Germany

© 2022 The Authors. European Journal of Organic Chemistry published by Wiley-VCH GmbH. This is an open access article under the terms of the Creative Commons Attribution License, which permits use, distribution and reproduction in any medium, provided the original work is properly cited.

transition rate constants increase approximately exponentially as the associated energy gap contracts,^[22] which generally decreases the quantum yield of photoisomerization in π -extended organic photochromes absorbing visible or NIR light.^[23] However, this disadvantage can be partially compensated, if molar absorption coefficients are high, making overall efficiency of this process large enough for practical use.^[24] Alternatively, the isomerization can be in certain cases efficiently performed using two (2P)-photon excitation or sensitization via photoinduced energy- or electron-transfer.

In the following section, we summarize the molecular design and resulting photophysical properties in selected classes of photochromic compounds that can isomerize within the visible range of light. While this section is by no means comprehensive, we want to particularly highlight examples of photochromes that have demonstrated the ability to undergo large bathochromic shifts due to chemical substitution.

2.1. Azobenzenes

Azobenzenes (AB) are among the most frequently applied molecular photoswitches.^[1d,25] Upon irradiation of the stable isomer (almost always with the *E*-configured —N=N— bond), they undergo photoisomerization to the thermodynamically unstable (or metastable) *Z*-isomer (In older sources, *trans*- and *cis*-configuration, respectively). For the unsubstituted AB, this process occurs upon exposure on UV light, and the reversible *Z*-to-*E* isomerization occurs quickly in presence of blue light, or upon thermal relaxation in darkness within several days. The unpolar *E*-AB ($\mu_D = 0$ D) has a planar conformation, whereas the *Z*-AB is strongly bent and possesses a higher dipole moment ($\mu_D \approx 3$ D).^[26] ABs have been incorporated into diverse functional scaffolds, such as biopolymers,^[25c,27] molecular machines^[28] or polymers^[29] The distinct advantage of azobenzenes is, that their photochromic properties including half-life, absorption wavelengths, switching rates, quantum yields, or the isomer ratio at photostationary states are broadly tunable upon structural modification. Numerous rapid and high-yielding synthetic protocols of the AB scaffold, developed industrially by over a century, are a considerable advantage in that process. Below, we present selected approaches to structural AB modifications, which led to visible light-activated compounds,

practically or potentially applicable in photoswitchable materials triggered without UV light.

2.1.1. Push-pull systems

The AB push-pull systems consist of an electron donating and an electron withdrawing group attached *para* to the azo bond on the opposite ends of the molecule.^[30] Such a substitution results in a considerable bathochromic shift of the absorption maxima, and thus enable *E-Z*-photoisomerization with visible light wavelengths (Figure 1a). However, these ABs have a very polarized structure, leading to significant solvato/acidochromism and short lifetimes of the *Z*-isomers.^[31] Furthermore, the mechanism of switching changed from linear transition (i.e. inversion) to rotation^[32] and the photophysical properties are often difficult to analyze as a result of the rapid thermal reversion. Another limiting factor for some applications (e.g. intramolecular crosslinkers for peptide functionalization) is the missing symmetry of push-pull ABs.

2.1.2. Tetra-ortho substituted azobenzenes

Substituents with heteroatoms (O, N, S) attached in the *ortho*-positions to the azo bond contribute a fraction of their nonbonding electron density to the aromatic systems, thereby lowering the energetic barrier for isomerization.^[30a,33] Bulky substituents in *ortho* position furthermore distort the planarity of the *E*-isomer, affecting the energy of both π and π^* molecular orbitals and resulting in the splitting of $n \rightarrow \pi^*$ bands of both isomers, which opens up a possibility to selectively excite each isomer with visible light frequencies – not possible for the unsubstituted AB due to overlap of the $n \rightarrow \pi^*$ bands. Earliest reported *ortho*-substituted ABs had amino groups as substituents. And while the substantial bathochromic shift and thermal stability (in the range of seconds) were obtained, more and more pronounced with increasing electron density, some of these compounds suffer from photobleaching (e.g. the green light-absorbing 2,2'-pyrrolidino derivative).^[34] To overcome this drawback, the Woolley's group synthesized fully visible-light-switchable tetra-*ortho* methoxy ABs (green light 80% *E*→*Z*, $t_{1/2}(Z) \approx 2.4$ days; and blue light 85% *Z*→*E*). Yet, this compound

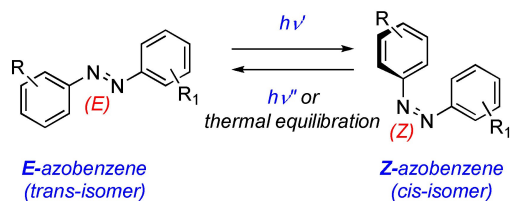


Anna-Lena Leistner received her Master degree in Chemical Biology from the Karlsruhe Institute of Technology in 2019. She is currently pursuing her PhD under the supervision of Zbigniew Pianowski also at the Karlsruhe Institute of Technology. Her research interest is focused on the development and analysis of diketopiperazine based photoswitchable materials.



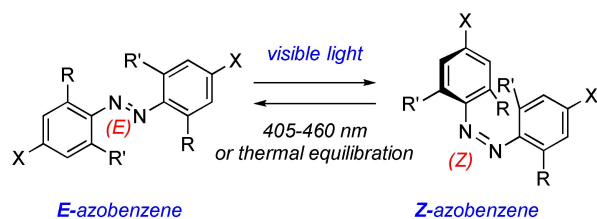
Zbigniew Pianowski received his PhD in chemistry in 2008 with Prof. N. Winssinger at ISIS ULP Strasbourg, working on artificial oligonucleotides. Then, he joined the group of Prof. D. Hilvert at the ETH Zürich as a Marie-Curie postdoctoral fellow, working in the area of protein engineering. Since 2014 he has been an independent group leader at the KIT Karlsruhe, where he habilitated in 2022. He also served as a deputy professor of organic chemistry at the University of Heidelberg (2017-2019). His research interests are focused on applications of molecular photoswitches in smart materials and biological systems.

a) Push-pull azobenzenes



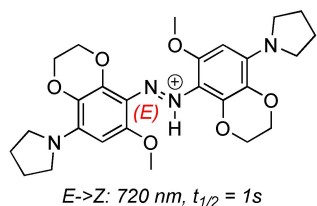
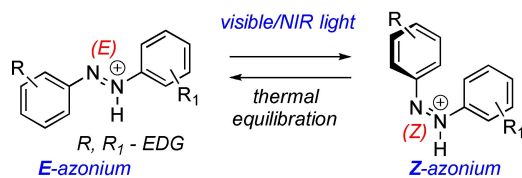
R	R'	$t_{1/2}$ (Z)	$\lambda_{\max}(E)$
-OC ₆ H ₁₁	-H	70 h	355 nm
-OC ₆ H ₁₁	-CN	6 h	375 nm
-OC ₆ H ₁₁	-NO ₂	24 min	375 nm
-N(C ₂ H ₅) ₂	-NO ₂	1.1 s	489 nm

b) Ortho-substituted azobenzenes

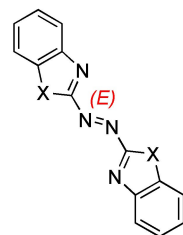
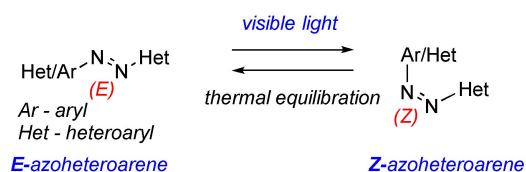


R	R'	X	$t_{1/2}(Z)$	E->Z
-F	-F	-H	ca. 700 d	530 nm
-OCH ₃	-OCH ₃	-H	2.4 d	530 nm
-Cl	-Cl	-H	21 h	635 nm
-F	-Cl	-H	12 h (70°C)	530-660 nm
-F	-F	-CHO, -C=C-	3.2 h (60°C)	>630 nm

c) Azonium switches

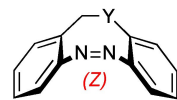
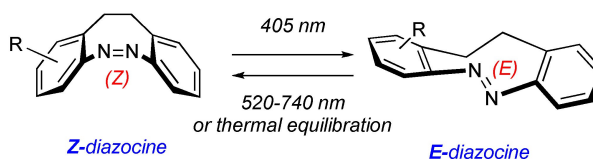


d) Azoheteroarenes



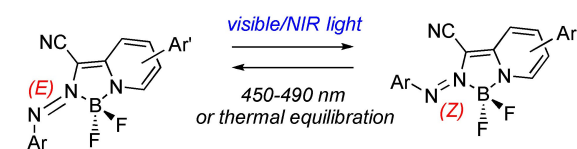
X	$t_{1/2}(Z)$	E->Z
azobis(2-Im)	175 s	408 nm
-NMe	520 s	488 nm
-O	14 s	488 nm
-S	0.4 s	488 nm
-NMe ⁺ TFA	280 s	591 nm

e) Diazocines



Y	$t_{1/2}(E)$	E->Z
-CH ₂ -	4.5 h	520 nm
-O-	89 s	520 nm
-S-	3.5 d	520 nm
-NAc-	29 min	525 nm
-NMe-	40 s	740 nm

f) BF₂-coordinated azobenzenes



R'	R''	$t_{1/2}(Z)$	E->Z
-H	-H	12.5 h	570 nm
-OCH ₃	-H	10.4 h	630 nm
-OCH ₃	-OCH ₃	13.4 h	640 nm
-N(CH ₃) ₂	-H	250 s	710 nm

Figure 1. Azobenzenes triggered with visible light (individual structures are depicted in their thermodynamically stable forms). a) Push-pull AB systems;^[30c,d,31] b) ortho-substituted azobenzenes;^[35–36,41–43] c) azonium switches;^[47] d) azoheteroarenes;^[53] e) bridged azobenzenes – diazocines;^[54–55] f) BF₂-coordinated azobenzenes.^[57–58]

was found to be sensitive ($t_{1/2} \approx 1.5 \text{ h}$ in 10 mM GSH) on glutathione – an intracellular reducing agent – and therefore

with limited application in a biological context.^[35] This problem has been solved with tetra-ortho thiol-substituted azobenzenes,

resistant on glutathione (up to 75% $E \rightarrow Z$ photoconversions, $t_{1/2}(Z)$ in the range of minutes, selected derivatives switchable with red light - 625 nm).^[33a] An alternative approach was to substitute the *ortho*-positions with halogen atoms. Woolley's group synthesized tetra-*ortho*-chloro ABs which are neither sensitive to photobleaching, nor to glutathione reduction, while the *E*-isomer shows the $n \rightarrow \pi^*$ transition band that can be excited with red light (to c.a. 85% *Z*-isomer at the PSS_{635 nm}), also *in vivo*.^[36] It was used i.e. in an antibiotic derivative to photocontrol antibacterial activity,^[37] or as a glutamate derivative ($t_{1/2}(Z) \approx 3.5$ h at 37 °C) - to control glutamate receptor ion channels.^[38] Broad range of potential applications stimulated development of new synthetic methods^[39] and detailed investigations of the photophysical properties.^[40] Concurrently, Hecht's group presented the outstandingly bistable tetra-*ortho* fluoro ABs (thermal *Z* to *E* relaxations in the range of years at room temperature) with high photoconversions (green light: 90% *Z*, and violet light: 97% *E*).^[41] Our group demonstrated, that their supplementary decoration with sp^2 substituents (-CHO, -C=C-) in the *para*-position results in additional bathochromic shift. These derivatives can be switched with red light (> 630 nm), with high photoconversions (82% *Z* with 660 nm, 85% *E* with 407 nm - for the *para*-bisaldehyde), although at the price of slightly lower thermal stability and decreased glutathione resistance ($t_{1/2} \approx 10$ h).^[42] Finally, combination of two chlorine and two fluorine atoms in the *ortho*-positions of AB ("dfdc-AB") resulted in high thermal bistability ($t_{1/2}(Z) = 16$ h at 70 °C) together with an increased $n \rightarrow \pi^*$ bands separation - which enables the $E \rightarrow Z$ switching with green (PSS_{530 nm}: 86% *Z*), but also red light (PSS_{660 nm}: 59% *Z*) (Figure 1b).^[43] Numerous materials bearing these azobenzenes have been, and will undoubtedly be developed in the near future.

2.1.3. Azonium switches

Azonium ions derived from amino-substituted ABs (like e.g. methyl orange) can efficiently absorb red light, and therefore be of potential interest for visible-light photoswitching. However, their low pKa values (typically in the range of 1.5–3.5) prevent the azonium species from being formed at neutral pH, and thus *in vivo* applications. And the short lifetime of the *Z*-isomers (μ s range) would require constant irradiation with strong light sources to achieve measurable long-lasting effects.^[44] The Woolley's group in 2013^[45] combined the *para*-amino and *ortho*-methoxy substitution pattern, which shifted the pKa to 7.2 and enhanced the thermal stability ($t_{1/2} \approx 10$ s upon irradiation with 635 nm, pH 7.5) without apparent photobleaching with moderate glutathione resistance ($t_{1/2} \approx 1.4$ h, 10 mM GSH). Changing some methoxy groups from the *ortho*- to *meta*-position and variation of the amino substituents resulted in far-red- and near-IR-excitable compounds, yet still with relatively short (μ s-s) lifetimes.^[45–46] The same group reported an AB with two *ortho*-methoxy groups and two *o,m*-fused dioxane rings (Figure 1c), which is protonated under physiological conditions, and can be isomerized with 720 nm

(near-IR) light to the *Z*-isomer with $t_{1/2} \approx 1$ s ($t_{1/2} \approx 3$ h in 10 mM GSH).^[47]

2.1.4. Azoheteroarenes

Azoheteroarenes are modified ABs, where one or both phenyl rings are replaced by heteroaromatic systems.^[48] They are far less studied than other AB derivatives, as their previous applications were long narrowed to strong nonlinear optic systems, and investigations of solvatochromism.^[49] Many of the primarily reported azoheteroarenes had short-living *Z* isomers. Yet, more recent investigations revealed their extended potential in tuning switching rates, degree of isomerization, or absorption frequencies.^[50] For example, in 2012, Herges' group presented *N*-substituted azoimidazoles with high thermal lifetimes and high photostationary states upon UV light irradiation for application as photodissociable ligands.^[51] And in 2014 Fuchter's group further improved this systems by additional substitution to prolong the half-life up to 1000 days. Several compounds, reported further by the same group,^[52] show impressive bistability and switching efficiency (bidirectionally to > 95% of each isomer). Though less thermally stable ($t_{1/2} < 10$ min), azobenzazoles reported by Beves group can be switched with blue (488 nm) light, and their protonation enables switching with yellow (591 nm) light without significantly compromising the thermal stability (Figure 1d).^[53] While the vast majority of reported azoheteroarenes needs UV light for isomerization, the high number of possible combinations of two heterocycles on the azo bond, as well as intense mechanistic investigations in the last decade rise reasonable hope for increasing the number of heteroarenes switchable without UV light, with high thermal stability and biocompatibility, and their application in smart materials.

2.1.5. Diazocines-bridged azobenzenes

The unusual photoswitching properties of diazocines (DAZ) - also known as bridged azobenzenes - were first reported in 2009 by Siewertsen *et al.*^[54] An AB was bridged in the *ortho* positions by a CH₂CH₂ linker. Due to the ring strain, and in contrary to previously discussed ABs, the thermodynamically stable form of DAZ is the *Z*-isomer (Figure 1e). The unsubstituted DAZ can be photoisomerized to the *E*-isomer (with the thermal lifetime $\tau = 4.5$ h at 28.5 °C) with violet light (> 90% *E* at the PSS_{400 nm}), and switched back to *Z* with green light (480–550 nm) with c.a. 100% efficiency.^[54] Later on, the Herges' group introduced also heteroatom-bridged diazocines. With oxygen and sulfur, the *E-Z* photoisomerization occurs with red light (660 nm), and with nitrogen (depending on the nitrogen's substituent) even with near-IR light with good conversion rates, quantum yields and thermal stability (e.g. for the *N*-acetylated nitrogen derivative: $t_{1/2} = 1.2$ h).^[55] Further investigations of the heteroatom-bridged diazocines yielded e.g. water-soluble compounds.^[56]

2.1.6. BF_2 -coordinated azo compounds

Complexation of the azo group with BF_2 , coupled with the extended conjugation of the $\text{N}=\text{N}$ π -electrons, results in another group of switches – “Azo- BF_2 ”. There, the increase in the energy of the $n\text{-}\pi^*$ transition and appearance of a new π -nonbonding (π_{nb}) to π^* transition that is well separated between the *E* and *Z* isomers enable efficient switching of the system with visible light (570/450 nm) with slow thermal relaxation rate of the *Z*-isomer ($t_{1/2} = 12.5$ h) (Figure 1f left, $\text{R}, \text{R}' = \text{H}$).^[57] Decoration of the phenyl ring with electron-donating substituents in the *para*- and *ortho*-position enabled efficient isomerization within the “therapeutic window” of light – in particular with NIR frequencies (Figure 1f left, $\text{R}, \text{R}' \neq \text{H}$).^[58] Replacing the quinoliny ring in azo- BF_2 switches with a phenanthridinyl one leads to emissive photochromic compounds whose emission can be photomodulated using visible light sources. Importantly, the thermal *Z*→*E* isomerization rate is strongly dependent on concentration, as a stabilizing self-aggregation through π - π interactions occurs.^[59] This effect is not observed anymore upon substitution with a methoxy group.^[60]

2.2. Indigoids

Indigo is one of the oldest known pigments, widely used in textile dyeing and renowned for its high (photo)stability.^[61] The central double bond of indigo does not undergo *E/Z* photoisomerization because of the excited-state proton transfer (ESPT).^[62] However, various classes of photoswitchable indigoids have been demonstrated (Figure 2a), including some fully addressable with visible light.

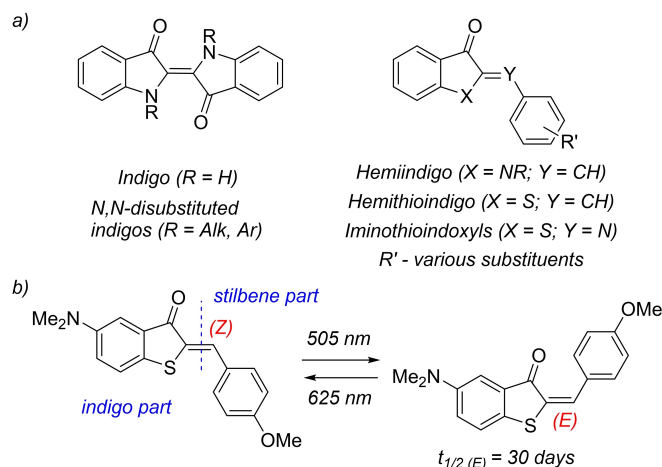


Figure 2. Indigoid photoswitches. a) the structures of non-photochromic indigo and related photochromic compounds originating from the indoxyl and thioindoxyl core;^[11] b) an example of hemithioindigo (HTI) photoisomerization, occurring mutually with green and red light.^[68]

2.2.1. Hemiindigos

In 1883 Adolf Baeyer first synthesized and reported hemiindigo (HI) – a hybrid of indigo and stilbene. But its photochromism remained unrecognized for over a century.^[63] Photochemistry of the parent hemiindigo is constrained by unwanted side reactions such as [2+2] cycloadditions or triplet generation. Some progress was made by installment of hydrogen bond donating groups on the stilbene part of HI. The hydrogen bonding stabilizes the *E*-isomer.^[64] In 2017, the group of Dube demonstrated bathochromically shifted push-pull systems via donor substitution – the indigo carbonyl assumes the acceptor part.^[65] These new HI derivatives are characterized by high bistability up to 83 years for some derivatives at 25 °C, high photoconversions, and addressability entirely with visible light – >90% *E*-isomers generated with 470–530 nm, and >90% *E*-isomers with 590–680 nm irradiation.

2.2.2. Hemithioindigos

Heimithioindigos (HTIs) – the combination of thioindigo and stilbene – are also photochromic compounds addressable with visible light.^[66] Donor substituents in the *para* position on the stilbene unit contribute to fatigue resistance,^[67] while the thermal stability of these derivatives is increased by additional donor-*para*-substituents (related to the sulfur) in the thioindigo fragment.

For the –OMe and –NMe₂ as the respective donors, efficient *Z*-*E* photoisomerization (up to 82% *E*-form with half-life of 30 days) can be achieved with blue or green light (470–505 nm), and the reverse process occurs with red light (up to 89% *Z*-isomer) (Figure 2b).^[68] And the bathochromic shift can be additionally enhanced – up to the amber (567 nm, >99% *E*) /near-IR (740 nm, 62% *Z*) photoisomerization – by electron-donating substituents with hydrogen bonding capacity.^[69]

HTIs with electron rich stilbenes and considerable pretwisting can adopt another state after photoexcitation, the twisted intramolecular charge-transfer (TICT) state, which provides a second deexcitation channel via rotation around the single instead of the double bond.^[70] These TICT states are highly polar. Thus, the light-induced event can be regulated by selecting either polar or non-polar solvents. The deep mechanistic analyses of the HTI scaffold^[71] resulted in numerous applications of the visible light triggered *E*-*Z*-isomerization,^[11] but also in a series of molecular motors based on the light-induced rotation.^[72]

2.2.3. *N,N'*-Disubstituted indigos

ESPT in the parent indigo inhibits photoisomerization.^[62] However, substitution at the nitrogen atoms results in photochromic compounds with tunable properties. Photochromism of *N,N*-dimethylindigo and its derivatives has been reported since mid-1950s.^[73] Later, the *N*-substitution effects have been studied – simple methylation or benzylation yields the most

distinct bathochromic shift (*E-Z* isomerization with 660 nm), but slightly lower thermal stability ($t_{1/2} < 5$ s in MeCN) than bis-*para*-methoxybenzyl ($t_{1/2} = 58$ s) or bis-*para*-nitrobenzyl ($t_{1/2} = 408$ min) substitutions.^[74]

2.2.4. Iminothioindoxyls

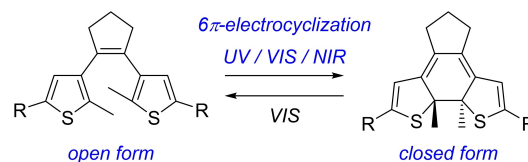
Iminothioindoxyl (ITI) switches - the hybrid of thioindigo and azobenzene - are accessible in one-step by condensation of thioindoxyl with substituted nitrosobenzenes. They show large band separation (> 100 nm) between photoisomers, glutathione resistance and isomerization in aq. solutions. The stable *Z*-isomers can be isomerized with blue light (455 nm) to the *E*-isomers with millisecond lifetime range.^[75]

Protonation of ITIs results in a bathochromic shift (λ_{max} 450–550 nm) and in contrary to most other protonated switches the half-life is increased to the range of seconds.^[36,76]

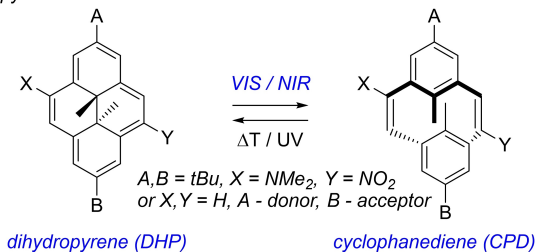
2.3. Diarylethenes

Diarylethenes (DAEs, Figure 3a)^[1e,77] undergo photoinduced cyclization and cycloreversion, therefore are suitable for applications where large changes in electronic properties or polarity are advantageous. Furthermore, they classify as P-type photoswitch by their thermal irreversibility and stand out by their high fatigue resistance. The classical DAE requires UV light activation for photocyclization. For visible light switching, several strategies are exploited.^[78] The first one – extension of the π -system^[79] – is limited by complex multi-step synthesis and low quantum yields. Moreover, in some cases total loss of photochromic activity was observed.^[80] The next approach is backbone modification: aromatic phosphole backbones with extended π -conjugation resulted in visible light responsiveness.^[81] Besides, DAE decorated with β -diketonate-ligands complexed with boron(III) resulted in NIR-switchable molecules with additional photoswitchable luminescence^[82] and pH sensing.^[83] Other approaches to adapt the photochromic properties of DAEs are: triplet sensitization,^[84] upconverting nanoparticles,^[23b] multiphoton absorption,^[85] or intramolecular proton transfer.^[86] The upconversion strategy relies on nanoparticles capable of absorption of multiple NIR photons and subsequent emission of shorter wavelength radiation. The initial demonstration with lanthanide-doped upconverting nanoparticles required physical separation of UV-light-emitting and green-light-emitting nanoparticles, as they were both activated with 980 nm IR light.^[23b] In the second NP generation, the emission wavelength could be tuned with the intensity of the excitation light.^[87] More recently, mesoporous silica-coated upconversion nanoparticles, with porphyrin photosensitizers covalently embedded inside the silica walls, and diarylethene photochromic switches loaded in the nanopores, have been used for NIR-controlled (980/808 nm) production of singlet oxygen (inhibited by the closed form of DAE).^[88]

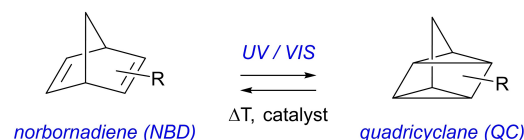
a) diarylethenes (DAE)



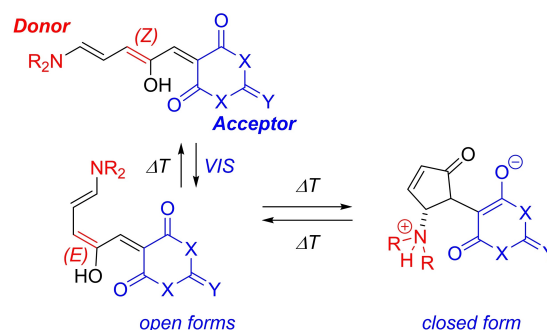
b) dihydropyrenes



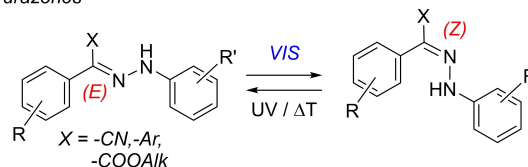
c) norbornadienes



d) Donor-acceptor Stenhouse adducts (DASA)



e) arylhydrazones



f) spiropyrans

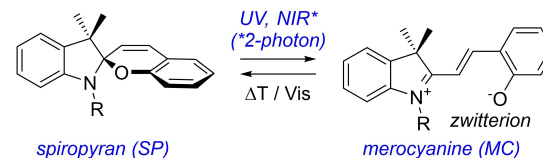


Figure 3. Other classes of photoswitches triggered with visible light – principles of the photoisomerization (thermally stable forms on the left side). a) diarylethenes,^[1e,77] b) dihydropyrenes,^[90] c) norbornadienes,^[101] d) donor-acceptor Stenhouse adducts,^[107b] e) arylhydrazones,^[114b] and f) spiropyrans.^[1f]

2.4. Dihydropyrenes

The photochromic behavior of dihydropyrenes (DHP, Figure 3b) was known since 1965^[89] and further investigated in more complex derivatives.^[90] DHPs are usually negative photo-

switches triggered with visible light. They undergo, with high conversions (>90%), a 6π cycloreversion to decolorized cyclophanedienes (CPDs) with long thermal lifetimes (often >24 h^[91]). Back-conversion to the fully aromatic form occurs thermally (T-type photoswitch) or upon UV light irradiation.^[92] The absorption of DHPs can be shifted to the red or NIR region by suitable donor-acceptor functionalization (a “push-pull” system).^[93] The absorption of the closed form and half-life of CPD are also highly solvent dependent, due to more distinct quinoid character in polar solvents.^[94] In cooperative switching in DHP dimers, the initial switching of first DHP unit enhances the quantum yield of the second switching of neighboring units.^[95] Another strategy applied for bathochromic shift of the DHP absorption maximum is to install heterocyclic substituents. Pyridine-substituted DHP can be switched to CPD with red light (>630 nm) upon protonation or formation of quaternary pyridinium salts. The back-isomerization occurred with UV light (365 nm) or thermally ($t_{1/2}$ >4 h).^[96] The pyridinium units can be additionally decorated with terpyridine residues, in various configurations. There, the following complexation of the ligands with Ru(II) ions does not affect the efficiency of the ring-opening photoprocess.^[97] Recently, it has been demonstrated that DHP systems decorated with bipyridine, in some cases complexed with Ru(II), can be reversibly switched with red (forward, to CPD) and blue (backward, to DHP) light.^[98]

2.5. Norbornadienes

Norbornadiene (Bicyclo[2.2.1]hepta-2,5-diene; NBD, Figure 3c) was first synthesized in 1950s by elimination of chlorine starting from 5,6-dichlorobicyclo[2.2.1]hept-2-ene^[99] or by condensation of cyclopentadiene with acetylene under pressure.^[100] The bicyclic ring system NBD undergoes UV-light-triggered [2+2] cycloaddition to the highly strained quadricyclane (QC). The QC photoisomer is metastable, has a high capacity of storing energy ($\Delta H = 89 \text{ kJ mol}^{-1}$)^[101] and reverts to NBD by heat or catalyst application and in this turn the stored energy is released. Due to this property NBDs are suited for application in solar energy storage, though the activation of parent NBD by UV light is a limiting factor.

2,3-substituted NBDs, accessible by Diels-Alder reaction (but limited to electron withdrawing residues), show absorption shifts to the visible light, but with concomitant decrease of their thermal stability.^[102] Diaryl-substituted NBDs, also switchable with visible light (<462 nm), have the thermal stability of the respective QCs in the range of days-to-months.^[103] Heteroaryl-linked NBD dimers switch below 468 nm (QC lifetime up to 16 h), but due to lower MW are better suited for solar thermal energy storage (increased energy storage capacity per mol).^[104] Dithiafulvalene linker can raise the absorption onset as high as 556 nm, but these compounds are more sensitive on photo-degradation, and photoisomerization reversibility is in some cases compromised.^[105]

2.6. Donor-acceptor Stenhouse adducts

Photochromism of donor-acceptor Stenhouse adducts (DASA, Figure 3d) was first reported by de Alaniz group in 2014.^[106] DASAs are T-type visible light photoswitches with negative photochromism (loss of color upon irradiation). They are characterized by rapid and modular synthesis based on furfural condensation with 1,3-dicarbonyl compounds. Upon the following ring opening with secondary amines, the conjugated, colorful, and hydrophobic form of the switch is obtained. Solvent-dependent, and thermally reversible switching occurs upon irradiation with visible light to produce the ring-closed, colorless zwitterionic cyclopentanone form.^[106] The switching mechanism is based on Z to E photoisomerization followed by conrotatory 4π -electrocyclization.^[107]

The high differences in hydrophobicity of the two DASA forms allow for dynamic phase transfer, which can be used e.g. for light-induced micellar delivery systems.^[108]

The 1st generation of DASA (alkylamines + barbituric/Meldrum's acid), which formed the closed isomer only in nonpolar aromatic solvents, showed high bond length alternation (BLA), and limited ability to tune wavelengths ($\lambda_{\text{max}} \sim 500 \text{ nm}$), was followed by the 2nd generation (arylamines + barbituric/Meldrum's acid, 2016), which enabled better spectral tuning (λ_{max} 400-700 nm), switching in more polar solvents (MeCN, EtOAc), and lower BLA, but compromised the thermodynamic equilibria (higher amount of the closed form in darkness).^[109] The 3rd DASA generation (2018, arylamines + more electron-withdrawing acceptors) enabled far-red activation and better control over the thermodynamic equilibria.^[110] However, in polar solvents (methanol, water), DASAs undergo irreversible ring closure.^[111] Inhibition of photoswitching with increasing photochrome concentration, observed in the 1st generation DASAs, has been recently addressed by introducing piperazine-based donors.^[112]

2.7. Hydrazones

Hydrazones (Figure 3e) are a class of molecular switches, that can be triggered with a variety of stimuli, like pH changes or metal ion coordination.^[113] Initial reports demonstrated UV-light-triggered photochromic aryl hydrazones.^[114] Further structural modifications of that scaffold enabled efficient Z→E photoisomerization with visible light (412–442 nm), and the back-isomerization triggered either with UV irradiation (340 nm) or thermally (very slowly, $t_{1/2}$ can reach 2700 years).^[115] The photophysical properties can be further tuned by substitution with electron-donating or -withdrawing substituents.^[116]

2.8. Spiroprans

Spiroprans (Figure 3f) are a class of multistimuli-responsive switches, usually obtained by condensation of salicylaldehydes with Fischer bases (methylene indolines), which react on photons, redox conditions, or changes in the temperature or

pH.^[117] The closed colorless form (SP) can isomerize to the (thermally unstable) colourful zwitterionic merocyanine (MC) – this was first observed thermally,^[117] and then also upon light irradiation.^[118] In presence of strong acids, photochromism is also recorded between *E*- and *Z*-isomers of the protonated merocyanine (MCH⁺).^[119] Bidirectional SP/MC switching can be induced on the picosecond timescale with high quantum yields.^[120] Spiropyrans have also high cross sections for two-photon absorption, and in some cases ring opening can be efficiently induced near-infrared light.^[121] However, the vast majority of SP cannot be photoisomerized with light above 400 nm. An alternative switching mechanism – oxidative dimerization – has been also reported for SP installed on gold surface as self-assembled monolayers.^[122] The chromism of spiropyrans, lifetime of particular forms, as well as other properties (e.g. hydrolytic stability) can be tuned in the broad range by modification of their substitution pattern.^[123] Spiropyrans and closely related spirooxazines^[124] exhibit also photo-switchable fluorescence, which can be used in superresolution microscopy. Due to their unique properties, spiropyrans have found applications in multiple dynamic materials.^[125]

3. Photochromic Materials Triggered with Visible Light

In the last two decades, a plethora of light-triggered smart materials based on molecular photoswitches have been reported. While majority of such materials are activated with UV irradiation, here we will present a selection of systems triggered with visible light. These are particularly profitable in such aspects, like: applicability in living organisms that are poorly penetrated with ultraviolet, deeper penetration of non-biological irradiated materials, materials propelled with sunlight, or systems with two (or more) orthogonal switches, independently activated with multiple wavelength frequencies for various functions. Below, we want to provide a subjective selection demonstrating the broad variety of systems and applications that can be achieved using visible light-triggered photoswitches.

3.1. Photo-responsive polymers

Stimuli-responsive polymers can react on small changes in the environmental conditions caused by physical, chemical, or biochemical stimuli. They have found numerous applications in the fields of biotechnology, medicine, and engineering. Photo-responsive polymers are particularly promising, as light can be applied with high spatiotemporal precision to elicit local effects.^[126]

The energy of visible light can be converted into mechanical oscillations with fluorinated azobenzenes incorporated into liquid crystal polymers (LCP), which combine the anisotropic character of LCs and the elasticity of rubbers. Fast, directed, and reversible actuation upon simultaneous illumination with blue

and green light (in dry or in aqueous environment) (Figure 4) is enabled by the presence of photoswitches, which transform the collective motions from the molecular-scale to the macroscopic level. Sunlight-propelled machines and self-cleaning surfaces are two most prospective applications of such materials.^[127]

Photoactuation can be used for light-driven interchange between various shapes. For that, a liquid crystal network (LCN) containing an azomerocyanine dye has been formed from polymerized mesogenic molecules. The resulting rewritable and reprogrammable single polymer film can generate various shapes upon irradiation with different colors of light (Figure 5).^[128]

Incorporation of molecular photoswitches into polymeric systems can be performed in a way that enables light to induce cyclic behaviors resulting in a directional macroscopic movement. For example, a millimeter-scale blue-light-powered (488 nm) inching walker, based on alignment-engineered liquid crystal elastomer film with an azobenzene component, can mimic the inching movement of a caterpillar and perform different locomotion on different substrates fueled by visible light at human-safe intensity levels.^[129] Or a hydrazone-based LCN film prone to photoinduced out-of-equilibrium macroscopic deformations, formed in a shape of four-blade plastic mill device, can convert focused light energy directly into mechanical work. Violet light-induced bending of the blades creates a force causing the rotation of the mill (Figure 6).^[130]

Other hydrazone-based actuators can drive chiral shape transformations in LCNs with violet light.^[131]

A visible-light-responsive bilayer actuator based on photoisomerization of DASA coupled to a poly(hexyl methacrylate) matrix was used to make a cantilever capable of lifting weight against gravity as well as a simple crawler. There, the negative photochromism and switching kinetics of DASA enabled tuning the thermal expansion and actuation performance of DASA-PHMA under constant light intensity. This enables the use of abundant broadband light sources to trigger tunable responses.^[132]

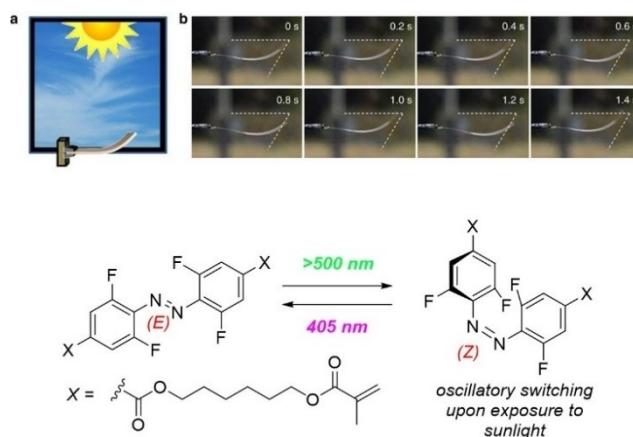


Figure 4. A liquid crystal polymer containing fluorinated azobenzene demonstrates oscillatory motion upon sunlight exposure. a) experimental setup; b) Series of snapshots extracted from the video depicting film oscillations. Reproduced from the ref.^[127]

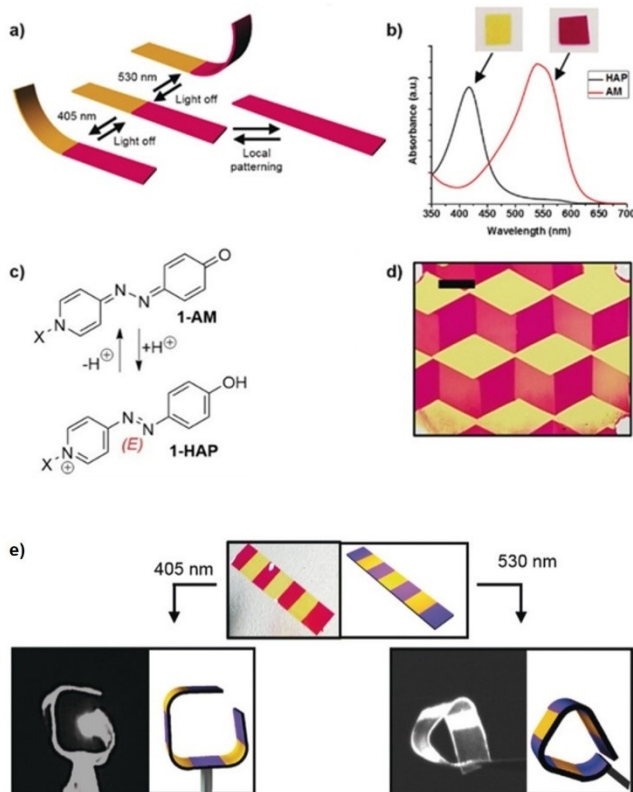


Figure 5. A reprogrammable and rewritable LCN-based polymer actuator. a) the yellow regions contain 1-HAP and the magenta regions contain 1-AM; b) Absorption spectra of the splay-aligned LCN polymer film before (1-AM) and after (1-HAP) acid treatment. Insets: The polymer film before and after acid treatment; c) Molecular changes upon acid and base treatment of 1-AM; d) Example of a pattern achieved with exposure to acidic vapor of a splay-aligned 1-AM LCN polymer film. Scale bar = 5 mm; e) specific bending of a patterned film. The same film is exposed with 405 nm (left) and 530 nm (right) light. The film specifically bends at the yellow region (with 405 nm) or at the magenta region (with 530 nm). Due to thermal reversibility, the film unbends to the flat state in darkness. Adapted with permission from the ref.^[128]

DASAs can be also non-covalently incorporated into a polymer film and induce deadhesion of the film from a glass surface by light-induced DASA ring-closure.^[133] The photoisomerization event has an effect on surrounding polymer chains, inducing nanoscale morphology changes. In comparison to previously demonstrated UV light-triggered adhesion modulation by polymers containing spiropyran or diarylethene photoswitches,^[134] the visible light (523 nm) used to trigger the DASA-containing polymer enabled deeper penetration of the material and decreased scattering. The process of deadhesion is not reversible due to inhibition of cyclization reaction at high DASA concentrations.^[135] Moreover, by dissolving the irradiated polymer films and thereby diluting the photoswitch, recovery of the open from proceeded rapidly.

DASA-containing polymeric materials can be also used as sensors, as exemplified by an on-off photoswitchable colorimetric method for the real-time detection of diethyl cyanophosphate (DCNP) – a nerve agent mimics (Figure 7). DASA chromophores and nucleophilic hydroxyl groups in the N-alkyl

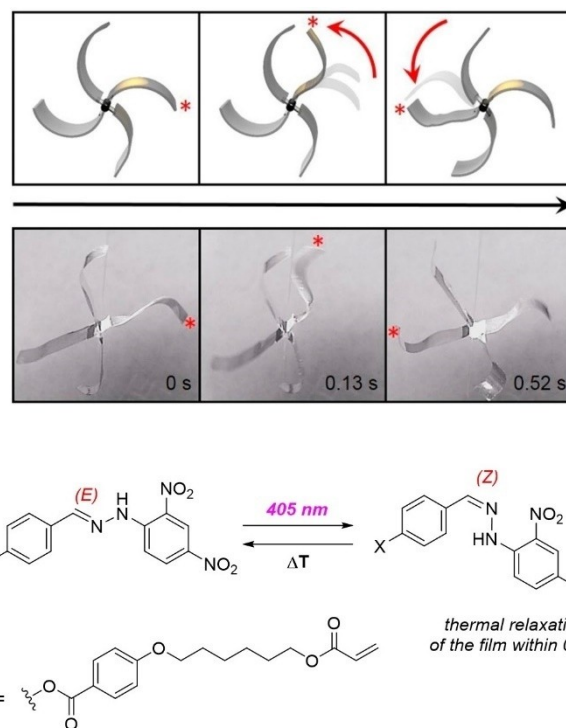


Figure 6. A four-blade light-propelled plastic LCN-based mill based on a hydrazone photoswitch. Schematic representation of the mill turning counterclockwise upon light irradiation (top). The light source (405 nm LED) is positioned on the top right of the mill and the focus point of the light is represented by a yellow spot on the right blade; Series of photographs showing time profiles of the rotation of the light-driven mill (bottom). Reproduced from the ref.^[130] Copyright (2017), with permission from Elsevier.

positions were incorporated into the polymeric backbone (GMA-co-DMA). Direct phosphorylation of the hydroxyl groups with DCNP and the subsequent intramolecular cyclization to form six-membered rings inhibits the DASA photoisomerization, yielding a rapid and selective colorimetric detection of DCNP in solution and in the vapor phase (with the latter detection achieved through the use of a DASA-derived spin-coated thin film).^[136] Fluorescent chemosensors for detection of metal ions (Fe^{3+} and Cu^{2+}) using DASA-functionalized polymer dots based on polyethyleneimines were also demonstrated.^[137]

Incorporation of molecular switches into polymers can result in multistimuli-responsive systems, such as a spiropyran-based flower that reversibly opens its petals and changes their colors upon stimulation with different light frequencies (Figure 8).^[138] Here, a monodomain/polydomain bilayer-structured liquid crystal elastomer (LCE) has been functionalized with two photochromic/thermochromic spiropyran units (upper layer) and a NIR-absorbing dye (bottom layer) to fabricate a trilight-modulated tricolor-changing flower mimic soft actuator. The resulting light-induced behavior is a combination of the photochromic effect, thermochromic effect, additive color blending effect, photothermal conversion effect, and gradient stress effect. Photochromism is responsible for the reversible color changes, while the shape deformation results from a photo-thermally induced LC-to-isotropic phase transition of the LCE –

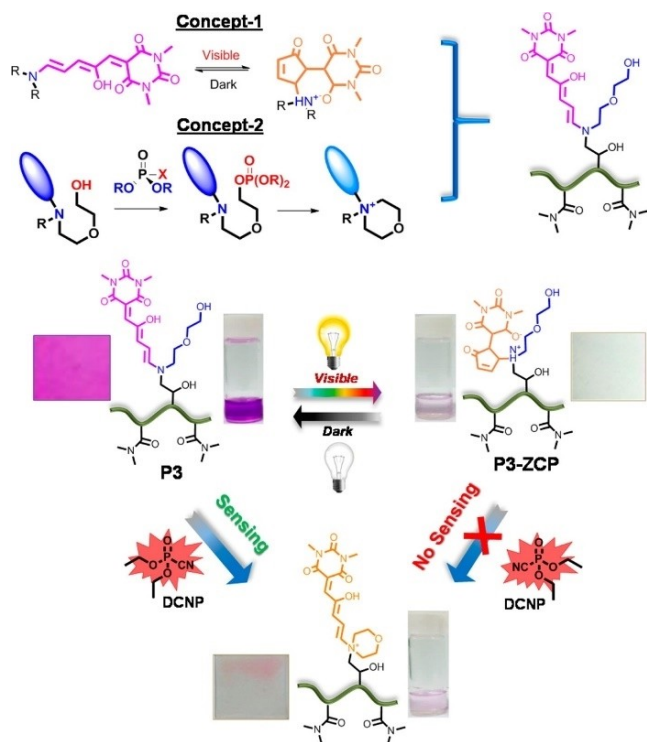


Figure 7. Schematic representation for a visible light-responsive polymeric system for the on-off colorimetric detection of a nerve agent mimics. The agent irreversibly blocks photochromism of the DASA scaffold. Reproduced with permission from the ref.^[136] Copyright (2016), with permission from American Chemical Society.

the difference in shrinking rate of both LCE layers upon NIR-induced heating generates gradient stress in the normal direction, which forces the LCE membrane to bend toward the upper layer. Additional color modulations have been achieved by adding further non-photochromic organic dyes, such as "Green 575".

The negative photochromism of dihydropyrenes (DHP) has been applied for visible light modulation of electronic conductance in a two-dimensional coordination polymer built from pyridine-functionalized dimethyl-DHP and Ag^I. The ON state of this system is characterized by the closed and planar DHP isomer with strong conductance. Visible light irradiation (456 nm) produces the CPD isomer, turning the switch OFF and reducing the conductivity drastically. Recovery of the ON state occurs by either heating or UV light irradiation (Figure 9).^[139] The pronounced difference in conductivity relies on the large change in the π -system from one continuous conjugated 30 π -electron system in the closed and redox active DHP form to two separated 14 π -electron systems in CPD form. Furthermore, these characteristics apply in solution state as well as thin films on indium tin oxide surface.

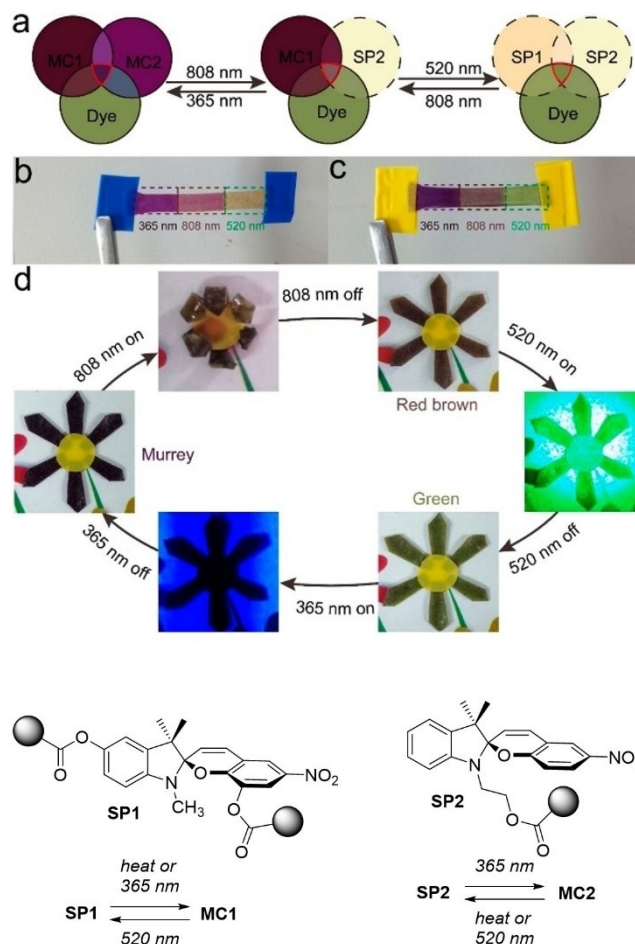


Figure 8. A tristable flower-like color-changing system. a) modulation by UV, green, and NIR light. Color appearances of three different regions of two liquid crystal elastomer films incorporated b) without or c) with Green 575 dye (0.5 wt%), exposed to UV, NIR, and green light; d) tricolor-changing flower with its blossom blooming and unblooming modulated by light with different wavelengths. Reproduced with permission from the ref.^[138] Copyright (2018), with permission from American Chemical Society.

3.2. Gels reacting on visible light

Hydrogels are soft material based on amphiphilic polymers (covalent or supramolecular), broadly applicable in the biomedical area, especially as implants, drug carriers, biosensors or contact lenses. Therefore, appending hydrogels with stimuli-responsiveness can broadly expand the scope of their biomedical applications. Photochromic gels can exhibit *e.g.* gel-sol phase transition, or light-induced changes of mechanical properties.

A supramolecular hydrogel based on two interwoven networks of polymers (polyacrylates) decorated with either β -cyclodextrin or tetra-*ortho*-methoxyazobenzene undergoes photoinduced gel-to-sol transition with red light (625 nm), using the fact that *E*- and *Z*-isomer differ in their affinity to the cyclodextrin. The reverse process occurred upon blue light irradiation (470 nm) or thermally. This material was used to

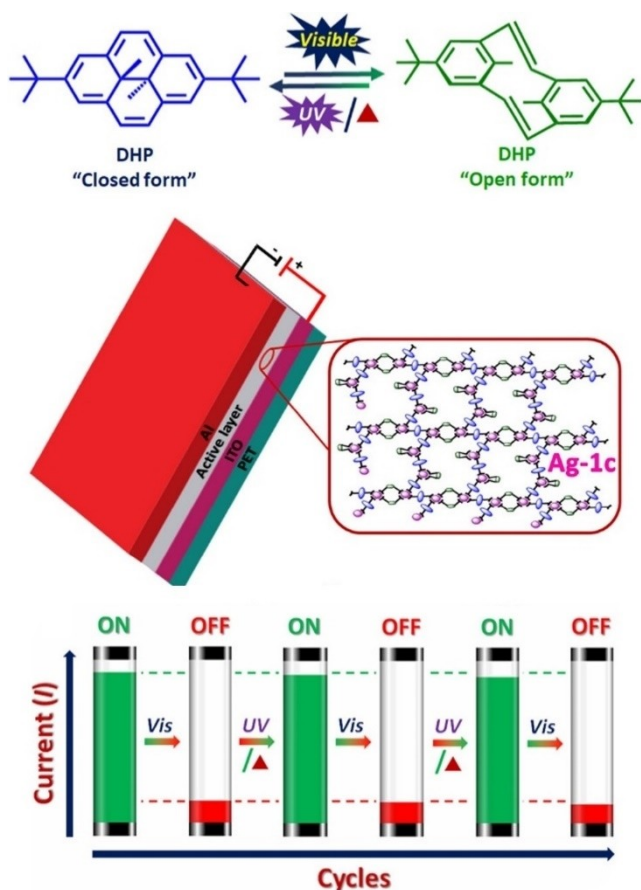


Figure 9. Photoinduced modulation of electric conductance based on reversible photoisomerization of the DHP-CPD (top); schematic representation of an ITO setup bearing the DHP-doped polymer (middle); variation of I upon alternate exposure to visible and UV light. The ON state (3.80 mA – green dotted line) and the photogenerated OFF state (0.67 mA – red dotted line) (bottom). Reprinted with permission from the ref.^[139] Copyright (2020), with permission from American Chemical Society.

encapsulate a fluorescently labelled protein (bovine serum albumin) and release it using red light.^[140]

Our group demonstrated low-MW supramolecular hydrogelators triggered with visible light based on *ortho*-fluorinated azobenzenes. The gels formed under physiological conditions can physically encapsulate a broad range of bioactive cargo molecules, such as antibiotics, anti-inflammatory, or anticancer drugs. Irradiation with green light (530 nm) results in a gel-sol transition with concomitant release of the cargo, while the gel can be reconstituted by violet light (410 nm). This system has been used to control bacterial growth with green light,^[141] as well as to release a potent low-nanomolar antimetabolic agent with high selectivity (Figure 10).^[142]

A polymeric hydrogel system based on the same *ortho*-fluorinated azobenzene switch, cross-linked with PEG polymer using click reaction, has been demonstrated. Photoisomerization with visible (green/blue) light reversibly changed its elastic modulus.^[143]

Photoinduced liquefaction occurs also in photochromic organogels, e.g. by photomodulation of stabilizing interactions

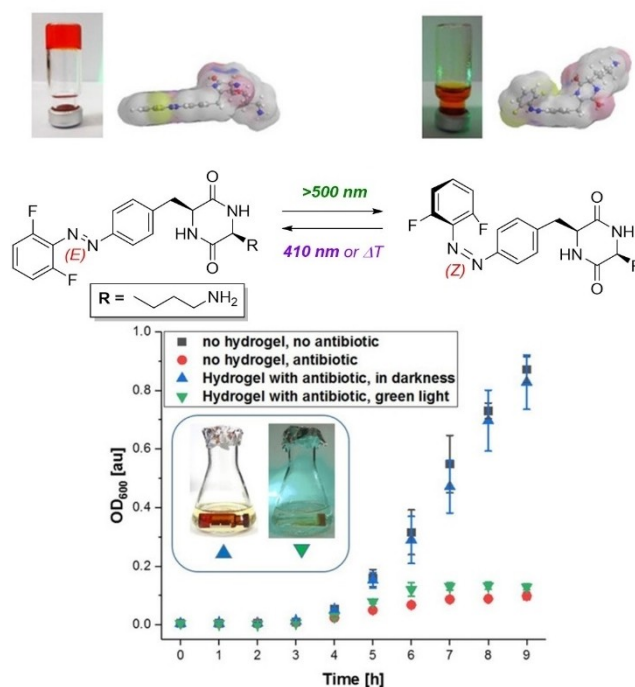


Figure 10. Supramolecular low-MW photochromic hydrogel (in phosphate-buffered saline PBS, pH 7.4) triggered with visible light. Irradiation with green light results in liquefaction, while violet light or heating restores the gel (top); physical loading of the hydrogel with an antibiotic (ciprofloxacin) and its subsequent phototriggered release enabled green light control over bacterial growth. Reprinted with permission from the ref.^[141]

between azopyridine and halogen bonds ($C_{Ar}-I$) on a mixed iodo/fluoroazobenzene. The green-light-induced liquefaction of the organogel (formed in THF) was reversible thermally, but not upon irradiation with other wavelengths.^[144] Full reversibility upon exposure on visible light frequencies was demonstrated in diazocine-based organogels (Figure 11) formed in hydrocarbons - they can be reversibly liquefied with violet or blue

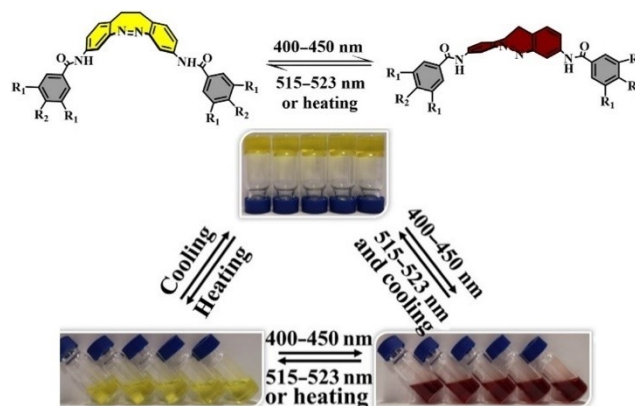


Figure 11. Diazocine-based organogelators. The chemical structure (top) and reversible liquefaction upon applying visible light frequencies (bottom). Reproduced with permission from the ref.^[145] Copyright (2021), with permission from Chinese Chemical Society.

light (400–450 nm) and solidified with green light (515–523 nm).^[145]

3.3. Molecular solar thermal energy storage

Molecular photoswitches can be also applied in the socially impactful area of renewable energies, to harvest solar energy in a non-photovoltaic manner. The concept of using photoswitches in molecular solar thermal energy storage (MOST)^[146] assumes accumulation of the metastable isomer by exposure to sunlight and following release of the stored energy in form of heat - by isomerization triggered with a catalyst.^[147] Several photoswitchable systems (anthracenes, stilbenes, azobenzenes, norbornadienes etc.) are investigated as candidates for MOST. The important criteria are: the absorbance of sunlight (UV and visible light), separated absorption bands of the isomers and pronounced bistability, a high storage enthalpy upon isomerization, energy release in form of heat triggered by an external stimulus (catalyst, electrochemically, light or heat) and overall stability of the system. As for now, the promising systems are based on norbornadiene (NBD) and azobenzene switches.

As the unsubstituted NBD is isomerized to QC by UV light, and thus only a small fraction of the spectrum provided by sunlight, its structure was intensively modified to identify derivatives with high bathochromic absorption shift. The main difficulties here were reduced thermal stability and increase in molecular weight, leading to a reduced energy storage density.^[148] These problems were addressed in more recent red-shifted NBD generations (various donor-acceptor substituent combinations).^[149] Currently, the best compromise between storage density, quantum yield, energy storage time and bathochromic absorption onset shift is achieved with the NBD-NBD dimers.^[150] Other concepts to maximize the solar energy transformation efficiency combine a MOST system with a flow reactor to heat water. There, up to 80% total efficacy of sunlight conversion was reached (Figure 12).^[151]

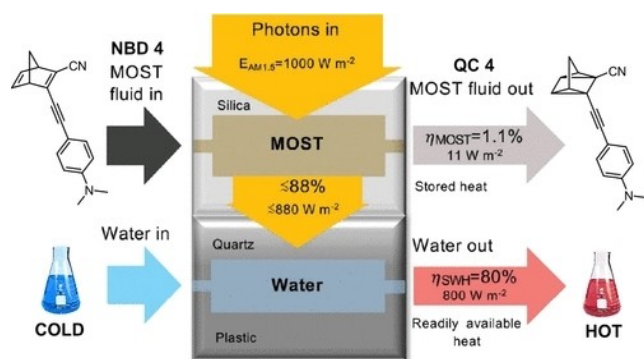


Figure 12. Hybrid solar energy conversion device. The upper side is used for photoisomerization of NBD, and the bottom side is used for water heating. Reproduced from the ref.^[149] Copyright (2020), with permission from American Chemical Society, and from the ref.^[151] Copyright (2017), with permission from the Royal Society of Chemistry.

Due to small geometric changes, phase transition upon switching of NBD to QC is not expected. This situation differs for AB photoswitches.

Combination of visible light-triggered *ortho*-substituted ABs as head groups and trideconate or ethylhexanoate groups as aliphatic tails leads to reduced melting temperatures of the materials. Thus, simultaneously to the isomerization from *E* to *Z* upon sunlight exposure, a phase transition from solid to liquid occurs (Figure 13).

The resulting liquid phase is characterized by exceptionally long (up to two months) latent heat and photon energy storage properties under a wide range of temperatures (−40 °C to 110 °C). The energy release in form of heat is triggered by short irradiation at 430 nm and accompanied by the reversed phase transition from liquid to crystalline.^[152]

3.4. MOFs and photochromic cages

Porous organic materials, such as metal-organic frameworks (MOFs), porous polymers, or porous carbonaceous materials are an emerging class of functional nanostructures with unusual properties, which found applications in storage, catalysis, electronic and proton conductivity,^[153] as sensors^[154] or for molecular separation,^[155] as well as in biomedical applications.^[156] Structural parameters of the pores are adapt-

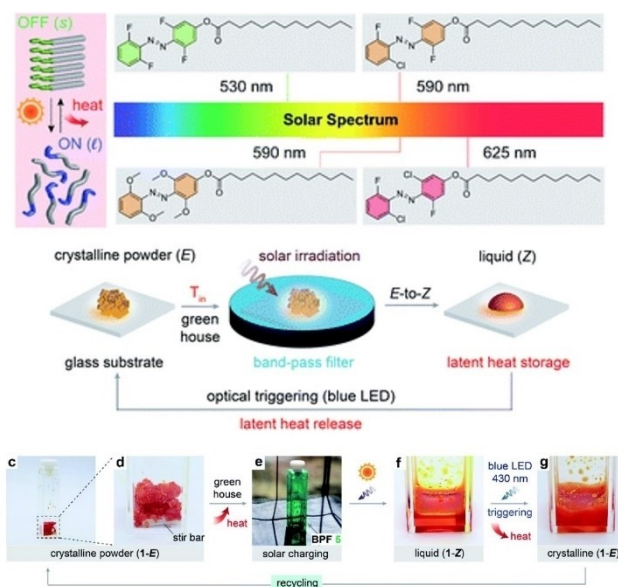


Figure 13. Photocontrollable phase-change materials. a) azobenzene derivatives triggered with visible light were functionalized as long-chain alkyl esters; b) a schematic illustration of the simultaneous phase transition and *E*-*Z* isomerization induced by the solar heat and visible-light-range solar irradiation through a band-pass filter. The initial crystalline *E* sample is regenerated after the optically-triggered heat release from the liquid *Z* by the blue LED (430 nm) irradiation; c)–g) the process of solar energy storage by a crystalline powder sample (1-*E*) in a magnetically-stirred container placed in a greenhouse. The entire sample turned liquid containing 72% *Z* isomer within 5 hours of exposure to sunlight at 31 °C ambient temperature. The liquid phase solidified within the 15 min exposure to blue LED light while being stirred for the uniform exposure. Reproduced with permission from the ref.^[152]

able in many ways by variation of pore volume, topology, surface area, resulting from the modifications of their chemical composition.^[157] Combination of photoswitches with porous materials enables dynamic transitions in these key characteristics and, consequently, opens the possibility to construct new classes of remotely controlled solids.^[158] It can be realized using three different methods: direct incorporation into the MOF/COF backbone,^[159] as a guest in the pores,^[158c] or as a covalent side chain on the backbone,^[160] whereby the latest is possible by post-synthetic modification or bottom-up synthesis.^[161]

The main advantage of introducing visible-light-triggered switches into porous materials instead of the unmodified UV-light activated ones are reduced photodegradation and increased penetration depth of the material.

A SURMOF – surface-mounted MOF – decorated with fluorinated ABs as side chains of the backbone was used to modulate membrane separation of hydrogen/hydrocarbon gas mixtures with alternating green and blue light.^[162] Another material based on fluorinated ABs – a two-component core-shell MOF^[158c] with a large porous interior – was constructed by solvent-assisted linker exchange of thin outer shell in the core-MOF crystals with AB-decorated linkers. In the solid state, this core-shell MOF shown reversible photoswitching with isomer ratios (PSS) comparable to the ligand in solution and without fatigue. These MOF crystals were subsequently loaded with a guest 1-pyrenecarboxylic acid, which was released in the configuration-dependent manner (Figure 14).

A different architecture was applied in case of a photochromic MOF composed of ZIF-8 crystals with angstrom-sized pore windows and specific cation binding sites, which non-

covalently encapsulated sulfonated spiropyrans. The nanometer-sized cavities of ZIF-8 can efficiently discriminate Li^+ from other alkali cations. Here, visible ($> 400 \text{ nm}$) light-triggered photoisomerization of the encapsulated spiropyran to the respective merocyanine resulted in photomodulation of the Li^+ conductivity through the material.^[163]

A water-soluble flexible coordination cage $\text{Pd}(\text{NO}_3)_2\text{tmeda}$ can influence the properties of encapsulated spiropyrans. The cage not only enhances water solubility of the guest, and stabilizes its otherwise unstable form, but also enables its reversible photoisomerization using blue light (460 nm) activation. This material has been implemented into two time-sensitive information storage media: a paper, on which writing can be performed using water as the ink, and a gel, which can be reversibly patterned using light (Figure 15).^[164]

The same coordination cage was also used as a host for different AB derivatives, to study their behavior in confined spaces. There, a cage containing fluorinated azobenzene, embedded in agarose gel, resulted in a material where an image can be written (using a mask) and erased by alternating irradiation with 520 nm and 420 nm light.^[158d,165]

3.5. Surfaces and nanoparticles

Self-organized attachment of reversibly switchable molecules to solid surfaces has recently attracted scientific interest in the field of advanced nanosystems, in particular potential applications as sensors,^[166] nanoelectronics^[167] or in optics (OLED).^[168] There are three important techniques to arrange the switches (i) chemisorption of self-assembled monolayers (SAMs) on metal surfaces, especially on gold (most often), (ii) Langmuir-Blodgett technique, and (iii) anchoring of guest molecules on the flat

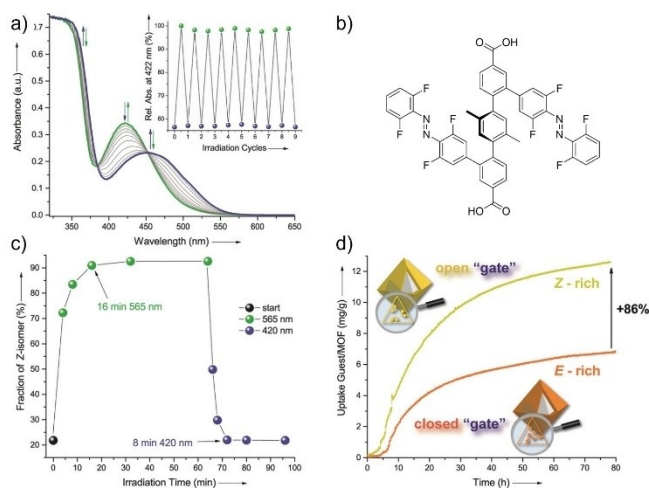


Figure 14. Modulating guest uptake in core-shell MOFs with visible light. a) Absorption spectra of solid Core-Shell-MOF II samples upon irradiation with green ($\lambda_{\text{irr}} = 565 \text{ nm}$) or blue ($\lambda_{\text{irr}} = 420 \text{ nm}$) light; the inset shows the relative absorbance at 422 nm over several switching cycles. b) chemical structure of bisazobenzene terphenyl linker; c) photoconversion after irradiation with green ($\lambda_{\text{irr}} = 565 \text{ nm}$) or blue ($\lambda_{\text{irr}} = 420 \text{ nm}$) light in solution; d) Uptake experiments of 1-pyrenecarboxylic acid by Core-Shell-MOF II for the different photoisomerization states of the shell (*E*-rich: 78% *E*-isomer content, *Z*-rich: 91% *Z*-isomer content) as monitored by UV/Vis spectroscopy. MOF particles were irradiated prior to the measurement. Adapted with permission from the ref.^[158c]

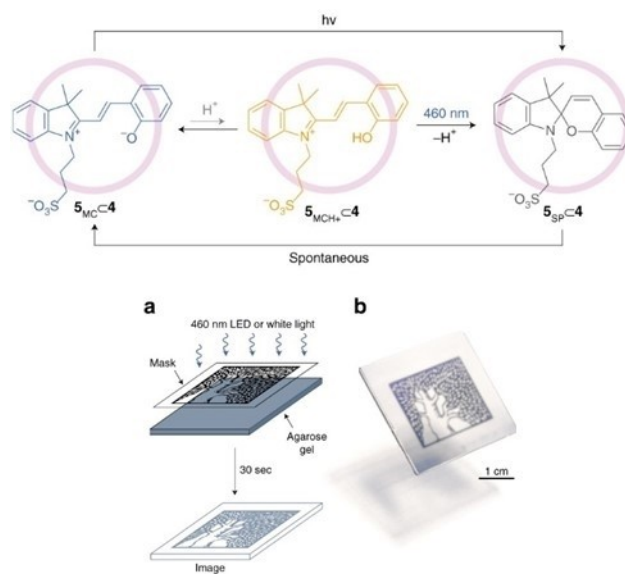


Figure 15. Photochromism of spiropyran in the cavity of a self-assembled cage, and self-erasing images engraved with blue light in a photoresponsive gel soaked with the inclusion complex. Reproduced from the ref.^[164]

facets of porous crystalline matrices. It is of major importance to have an adequate spacing and geometry between photochromic molecule and metal surface due to quenching of excited states by the metal.^[169] Common spacer groups to form SAMs are alkylthiols, though they often do not provide sufficient volume availability for the photoisomerization process on the surface.^[170]

DASA is a promising switch for surface applications, due to its negative photochromism, as well as its large conformation and polarity changes upon photoisomerization induced with visible light. Functionalization of the surface of a polycarbonate foil with *in situ* synthesized DASA, enabled visible-light-triggered, however irreversible, photopatterning of the surface.^[171] DASA-functionalized nanoparticles were also prepared, based on a catechol anchor with affinity to Fe₃O₄ nanoparticles. However, irreversible bleaching has been observed instead of the reversible isomerization.^[172] In both cases, the irreversible process is a result of lateral stabilization of the zwitterionic isomer of surface immobilized DASAs.

Recently, the first example of DASAs with maintained functionality on metal surfaces was demonstrated with DASA-covered gold nanoparticles. The pronounced polarity change upon isomerization of DASAs can cause effects upon nonlinear colloidal stability and reversible self-assembly of nanoparticles (Figure 16).^[173]

There, the reversible switching was possible when 1-undecanethiol (UDT) was added as co-ligand. With the composition of 50% UDT and 50% of the 11-thio-*N*-DASA, the back-switching was not observed, while upon increasing the UDT content to 90%, the chromophore behaved as one freely diffusing in the solution. Its isomerization occurred reversibly over 6 min per cycle, without any considerable fatigue. In this system, with the right composition of co-ligand and spacer length an enlargement of the interligand space was observed, enabling solvation of the ligands, and cancelling the attractive interactions between them. As a result, the polarity of the nanoparticles increased and more pronounced effects on aggregation were observed upon irradiation with green light (570 nm).

The problem of volume availability has been also addressed with molecular platforms built from triazatriangulenium (TATA) or trioxatriangulenium (TOTA) – large π -systems with high affinity (in the same range as thiol-Au bonds) to flat gold surfaces. The required volume availability is controllable by selection of appropriate substituents. The TATA/TOTA platforms enable installation of ABs^[174] and NBDs^[175] on gold surfaces in upright vertical orientation, as well as lateral installation of ABs – an approach which was rarely reported before.^[176] TATAs linked with fully visible light switchable diazocines^[177] were developed and its photochromism investigated after assembly on Au^[11] surfaces. In both cases – azobenzenes and diazocines – a significant decrease in thermal stability was observed for the metastable photoisomer. This was explained with a very peculiar thermal singlet-triplet-singlet mechanism^[177] mediated by bulk gold via a conjugated system with 11 bonds and a distance of 14 Å.^[178] This phenomenon is described as “spin-switch catalysis”.

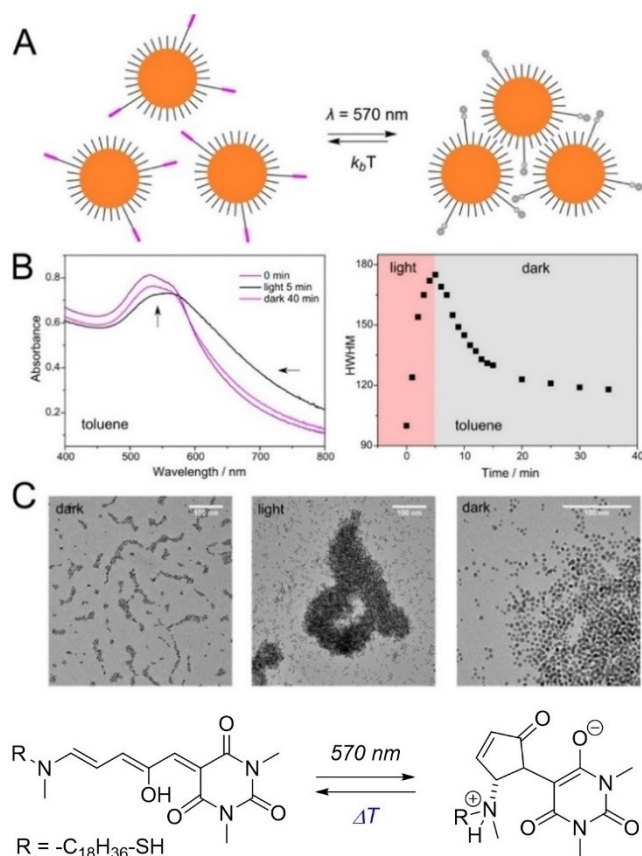


Figure 16. Light-induced reversible self-assembly of gold NPs covered with a DASA-functionalized alkanethiols: A) cartoon representation, B) absorbance spectra and kinetic traces, C) TEM micrographs, and D) structure of the used switch. Photograph on right depicts blurring of initially sharp edges of an NP aggregate due to the detachment of the NPs under thermal relaxation in the dark. Reproduced from the ref.^[173] Copyright (2021), with permission from American Chemical Society.

Another example of visible-light-triggered aggregation has been demonstrated using cyclodextrin-coated lanthanide-based upconverting nanoparticles (UCNPs) and bifunctional linkers decorated with azobenzenes and arylazopyrazoles. UCNPs absorb several low energy photons and in return emit a high energy photon. In result, near-infrared light (980 nm) can be used to induce the *E*→*Z* photoisomerization, which in turn controls the formation of respective host-guest complexes and the resulting aggregation. The aggregate dissipation occurs upon 450 nm light irradiation and the following *Z*→*E* isomerization of the azo compounds.^[179]

Photomodulation of electronic energy levels creating “opto-electronic devices” can be achieved by hybrid organic/inorganic semiconductor structures. However, most known hybrid structures are featuring DAE, AB or SP, and most of these switches are reactive on UV light. Furthermore, their isomerization is accompanied by large structural changes. These properties are major drawbacks for solid state devices since there is susceptibility to photodegradation upon UV light irradiation and densely packed structures sterically hinder geometrical changes.

A photochromic hybrid organic/inorganic semiconductor interface was demonstrated by anchoring pyridyl-DHP to the inorganic semiconductor ZnO.^[180] As negative T-type switch, pyridyl-DHP is switched to its open form by green light (565 nm) and can be reversed to the closed form by mild heat (50 °C). When anchored to ZnO, the pyridyl-DHP layer can reversibly modify the electronic properties of ZnO surfaces. Upon photoisomerization, the molecular orientation of the pyridyl-DHP is changed from standing up to laying down accompanied by different ionization energies. As a result, a reversible shift of frontier occupied molecular levels by 0.7 eV with respect to the Fermi level was observed.

3.6. Other systems

Lab-on-a-chip devices recently attracted a lot of attention – both in academia and industry – as they deliver various functionalities with high throughput and low sample amounts. Powered fluid flow is usually achieved with mechanical, electrokinetic, or chemically powered systems.^[181] However, technical challenges, requirement for external power supply, or inability of precise deactivation methods make a demand for more precise solutions.

The versatility provided by visible-light addressable photo-switches offers a new basis for autonomous control of liquid flow, as demonstrated by a system where DASAs are applied to control fluid flow in a dynamic and self-regulating way, by means of photo-controlled Rayleigh-Bénard convection (Figure 17).^[182]

The highly tunable switching kinetics of the third generation DASA built from a CF₃ pyrazolone-based acceptor and a 2-methyl indoline donor (DASA-CF₃-PI) enabled construction of an experimental setup for localized fluid motion. A photothermal gradient is built by short irradiation with a red-light LED focused to a point of interest, creating an advection pathway for particles. In other words, an upwards flow based on buoyancy effects is established independent from the spatial orientation of the light source. In addition, the flow continues when the light source has been removed, enabling thermal reverse isomerization of the DASA to the colored open form and thereby the opportunity to direct particles along multiple trajectories.^[182]

Visible light can also trigger changes in photoresponsive helical superstructures of liquid crystals. In cholesteric liquid crystals formed by addition of photochromic dopants into nematic liquid crystals, it is possible to either induce reversible phase transition or handedness inversion with light. In the discussed example, achiral nematic liquid crystals with cyano groups readily form halogen-bonding complexes with a photoresponsive chiral dopant – an AB-based photoswitch with bromine or iodine substituents. (Figure 18).^[183]

Depending on the halogen atom used, the cholesteric liquid crystal either reacted by reversible handedness inversion or cholesteric-nematic phase transition upon green and blue light irradiation (Figure 19).^[183]

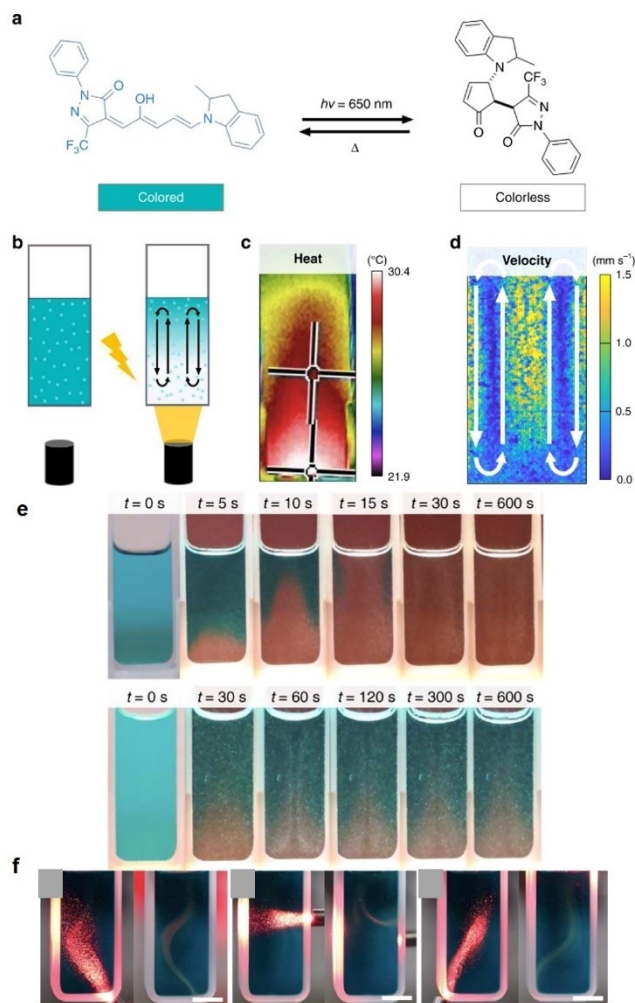


Figure 17. DASA for autonomous control of liquid flow. a) DASA-CF₃-PI switching under visible light irradiation from an extended, colored, open form to a compact, colorless, closed form; b) Schematic of experimental setup for convective particle tracking. Light shone on the bottom of a quartz cuvette causes DASAs to switch to the colorless form, while also generating c) heat gradients and d) fluid flows due to convection in toluene; e) bleaching front progression through 0.25 mM DASA-CF₃-PI in chloroform stabilized with 0.75 % ethanol (top) and toluene (bottom) irradiated with 25 mW cm⁻² light; f) spatially precise convective flows: irradiating one portion of the cuvette using a red LED light, and convective flows that ensue due to irradiation (on the left and right side of each panel a-c, respectively). Reproduced from the ref.^[182]

DASAs have been also explored as possible visible-light-triggered actuators for photoswitching in liquid crystalline systems. Upon irradiation with 532 nm light, DASA induces a rapid and reversible phase transition within a phytantriol-based liquid crystalline system, with the impact on phase behavior being dependent on the concentration of DASA. The photochemical behavior of the DASA component in this liquid crystalline environment, however, was not straightforward, comprising some irreversibility in the photoswitching process, which was partially assigned to a photothermal effect.^[184] In another experiment, lipid-based lyotropic liquid crystalline system doped with DASA performed a rapid and fully reversible phase transition from lamellar to inverse cubic phase upon

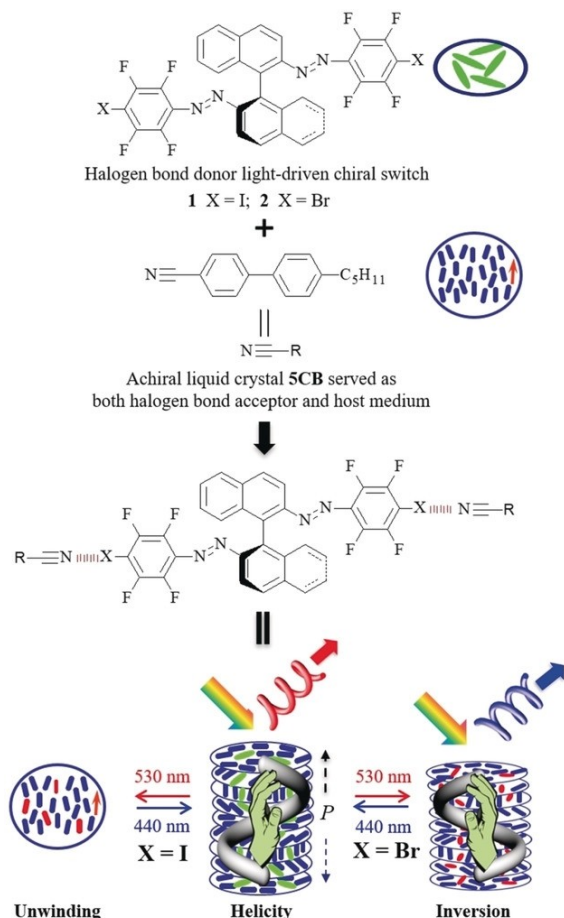


Figure 18. Photomodulation of liquid crystal properties with visible light. *Top:* Chemical structures of visible-light-driven, halogen bond donor based, chiral molecular switches (S)-1 and (S)-2 and the achiral nematic LC 5CB, which functions as both the halogen bond acceptor and host medium. *Bottom:* Schematic representation of reversible unwinding and handedness inversion in the self-organized helical superstructure upon visible-light irradiation. Reproduced with permission from the ref.^[183]

irradiation with green light (532 nm), reverting back on removal of light. Irradiation can trigger a burst release of a previously encapsulated fluorescent cargo (a dextran-fluorescein conjugate) upon phase transition, as a model for more complex visible-light-activated drug delivery systems.^[185]

3.7. Biological applications of visible-light photochromism

Although this Review is focused primarily on photochromic materials, which are operational within the visible range of light, it has to be underlined that another broad application field for visible-light-triggered photoswitches are biological systems. Better penetration of cells and tissues with visible light, as well as lower scattering and less photodamage in comparison to UV light^[18] constitute the most obvious advantages. Superresolution microscopy is an excellent tool for imaging both materials^[186] and biological systems.^[187] Structural optimization of photoswitchable fluorophores^[188] towards compatibil-

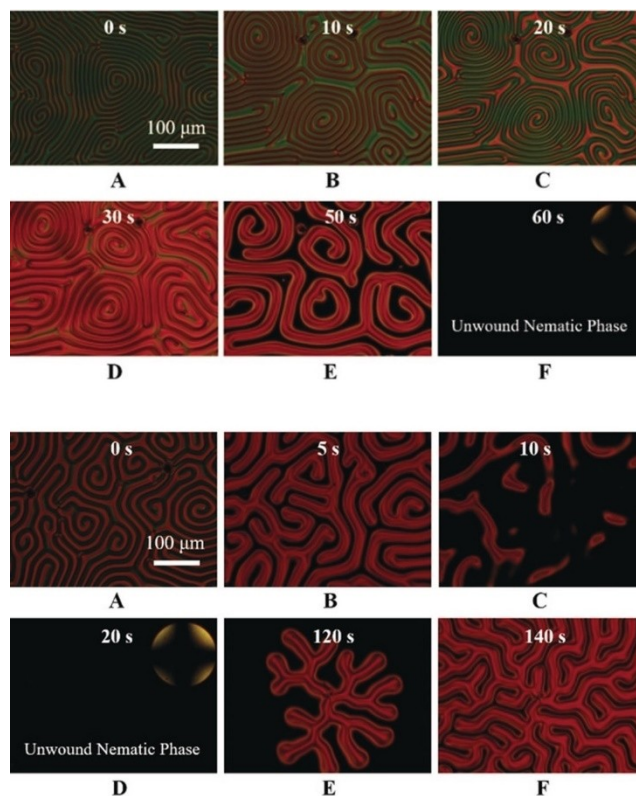


Figure 19. Polarization microscopy images of (top) cholesteric liquid crystals containing 1.0 mol % of 1, showing the transition to the nematic phase upon 530 nm light irradiation; and (bottom) handedness inversion (1.0 mol % of 2) upon 530 nm light irradiation (both in a homeotropic cell). Reproduced with permission from the ref.^[183]

ity with aqueous environment^[189] and activation with visible light (e.g. in spirooxazines^[190] or diarylethenes^[191]) could expand the scope of this technology in complex biological setups.^[192] Optogenetics is a technique to control activity of neurons or other cell types with light, by expression of light-sensitive ion channels, pumps, or enzymes.^[193] The analogous effect – photocontrol of ion channel activity – can be achieved with molecular photoswitches.^[17b,194] There, an ambitious goal is vision improvement or restoration to the people suffering from macular degeneration or degenerative retinal diseases.^[195] Several visible-light-triggered, mostly azobenzene-based photochromic systems have been developed and optimized for the ion channel activity photomodulation.^[38,196] In parallel, methods of two-photon excitation of the azobenzene chromophore have been developed to enable deep tissue activation with NIR light.^[197]

Visible-light-triggered photocontrol over conformation or activity of biomolecules such as peptides,^[14,27b,198] peptidomimetics,^[199] proteins,^[200] oligonucleotides,^[201] oligosaccharides,^[202] and lipids^[39a,203] has been also successfully demonstrated.

Light frequencies above 600 nm (red and NIR-light) can deeply penetrate soft tissues of the human organism due to low absorption by blood hemoglobin. Thus, implementation of red- and NIR-activated photoswitches in pharmacophores, as

demonstrated with red light-triggered photoswitchable antibiotics,^[37,198] are particularly important for the advancement of photopharmacology.^[17] Another challenge there is the switch compatibility with aqueous environment.^[6]

4. Summary and Outlook

In this Review, we have discussed several classes of molecular photoswitches that can be photoisomerized without using of the UV light – entirely, or in particular structural modifications. Then, we selected a number of their representative applications in various types of materials, which function and behavior is triggered or modulated with visible light. The selection is far from comprehensive, due to the limited manuscript size, but it was intended to provide a realistic impression on the scope, advantages, and existing limitations of such materials.

Acknowledgements

The authors gratefully acknowledge the financial support from Deutsche Forschungsgemeinschaft (DFG) in form of an individual grant PI 1124/6-1 and PI 1124/6-3, as well as participation in the Graduate Training School (Graduiertenkolleg) GRK 2039 and the YIN Grant of the KIT Karlsruhe. A.-L. L. is grateful to the Land of Baden-Württemberg for the support in form of “Landesgraduierstipendium”. We want to thank Prof. Dr. Stefan Bräse (KIT Karlsruhe) for the infrastructural support. Open Access funding enabled and organized by Projekt DEAL.

Conflict of Interest

The authors declare no conflict of interest.

- [1] a) Z. L. Pianowski, *Chem. Eur. J.* **2019**, *25*, 5128–5144; b) J. D. Harris, M. J. Moran, I. Arahamian, *Proc. Natl. Acad. Sci. USA* **2018**, *115*, 9414–9422; c) D. Cameron, S. Eisler, *J. Phys. Org. Chem.* **2018**, *31*, e3858; d) H. M. Bandara, S. C. Burdette, *Chem. Soc. Rev.* **2012**, *41*, 1809–1825; e) M. Irie, T. Fukaminato, K. Matsuda, S. Kobatake, *Chem. Rev.* **2014**, *114*, 12174–12277; f) L. Kortekaas, W. R. Browne, *Chem. Soc. Rev.* **2019**, *48*, 3406–3424; g) D. Lachmann, R. Lahmy, B. König, *Eur. J. Org. Chem.* **2019**, *2019*, 5018–5024; h) M. M. Russew, S. Hecht, *Adv. Mater.* **2010**, *22*, 3348–3360; i) C. Petermayer, H. Dube, *Acc. Chem. Res.* **2018**, *51*, 1153–1163.
- [2] H. Bouas-Laurent, H. Dürr, *Pure Appl. Chem.* **2001**, *73*, 639–665.
- [3] A. Cembran, F. Bernardi, M. Garavelli, L. Gagliardi, G. Orlandi, *J. Am. Chem. Soc.* **2004**, *126*, 3234–3243.
- [4] B. Heinz, S. Malkmus, S. Laimgruber, S. Dietrich, C. Schulz, K. Ruck-Braun, M. Braun, W. Zinth, P. Gilch, *J. Am. Chem. Soc.* **2007**, *129*, 8577–8584.
- [5] S. Aiken, R. J. L. Edgar, C. D. Gabbutt, B. M. Heron, P. A. Hobson, *Dyes Pigm.* **2018**, *149*, 92–121.
- [6] J. Volaric, W. Szymanski, N. A. Simeth, B. L. Feringa, *Chem. Soc. Rev.* **2021**, *50*, 12377–12449.
- [7] I. M. Welleman, M. W. H. Hoorens, B. L. Feringa, H. H. Boersma, W. Szymanski, *Chem. Sci.* **2020**, *11*, 11672–11691.
- [8] R. Dorel, B. L. Feringa, *Chem. Commun. (Camb.)* **2019**, *55*, 6477–6486.
- [9] W. C. Xu, S. Sun, S. Wu, *Angew. Chem. Int. Ed. Engl.* **2019**, *58*, 9712–9740.
- [10] A. Goulet-Hanssens, F. Eisenreich, S. Hecht, *Adv. Mater.* **2020**, *32*, e1905966.
- [11] W. Danowski, T. van Leeuwen, W. R. Browne, B. Feringa, *Nanoscale Adv.* **2021**, *3*, 24–40.
- [12] a) P. F. Luo, S. L. Xiang, C. Li, M. Q. Zhu, *J. Polym. Sci.* **2021**, *59*, 2246–2264; b) J. Boelke, S. Hecht, *Adv. Opt. Mater.* **2019**, *7*, 1900404; c) L. Li, J. M. Scheiger, P. A. Levkin, *Adv. Mater.* **2019**, *31*, e1807333.
- [13] O. Galangau, L. Norel, S. Rigaut, *Dalton Trans.* **2021**, *50*, 17879–17891.
- [14] L. Albert, O. Vazquez, *Chem. Commun. (Camb.)* **2019**, *55*, 10192–10213.
- [15] S. Maisonneuve, C. Lin, J. Xie, *Vietnam J. Chem.* **2020**, *58*, 417–422.
- [16] W. Szymanski, J. M. Beierle, H. A. Kistemaker, W. A. Velema, B. L. Feringa, *Chem. Rev.* **2013**, *113*, 6114–6178.
- [17] a) W. A. Velema, W. Szymanski, B. L. Feringa, *J. Am. Chem. Soc.* **2014**, *136*, 2178–2191; b) K. Hull, J. Morstein, D. Trauner, *Chem. Rev.* **2018**, *118*, 10710–10747.
- [18] a) R. Weissleder, V. Ntziachristos, *Nat. Med.* **2003**, *9*, 123–128; b) R. R. Anderson, J. A. Parrish, *J. Invest. Dermatol.* **1981**, *77*, 13–19; c) R. Weissleder, *Nat. Biotechnol.* **2001**, *19*, 316–317.
- [19] P. Kamarajan, C. C. Chao, *Biosci. Rep.* **2000**, *20*, 99–108.
- [20] K. Grill, H. Dube, *J. Am. Chem. Soc.* **2020**, *142*, 19300–19307.
- [21] R. Weinstein, T. Slanina, D. Kand, P. Klan, *Chem. Rev.* **2020**, *120*, 13135–13272.
- [22] S. J. Jang, *J. Chem. Phys.* **2021**, *155*, 164106.
- [23] a) in *Photochemistry of Organic Compounds*, **2009**, P. Klán, J. Wirz, pp. 25–72; b) C. J. Carling, J. C. Boyer, N. R. Branda, *J. Am. Chem. Soc.* **2009**, *131*, 10838–10839.
- [24] T. Solomek, J. Wirz, P. Klan, *Acc. Chem. Res.* **2015**, *48*, 3064–3072.
- [25] a) F. A. Jerca, V. V. Jerca, R. Hoogenboom, *Nat. Chem. Rev.* **2021**, *6*, 51–69; b) A. A. Beharry, G. A. Woolley, *Chem. Soc. Rev.* **2011**, *40*, 4422–4437; c) R. J. Mart, R. K. Allemann, *Chem. Commun. (Camb.)* **2016**, *52*, 12262–12277.
- [26] G. S. Hartley, R. J. W. Le Fèvre, *J. Chem. Soc.* **1939**, *0*, 531–535.
- [27] a) N. Preusske, W. Moormann, K. Bamberg, M. Lipfert, R. Herges, F. D. Sonnichsen, *Org. Biomol. Chem.* **2020**, *18*, 2650–2660; b) S. Samanta, C. Qin, A. J. Lough, G. A. Woolley, *Angew. Chem. Int. Ed. Engl.* **2012**, *51*, 6452–6455.
- [28] a) T. Hugel, N. B. Holland, A. Cattani, L. Moroder, M. Seitz, H. E. Gaub, *Science* **2002**, *296*, 1103–1106; b) S. Muramatsu, K. Kinbara, H. Taguchi, N. Ishii, T. Aida, *J. Am. Chem. Soc.* **2006**, *128*, 3764–3769; c) A. S. Lubbe, Q. Liu, S. J. Smith, J. W. de Vries, J. C. M. Kistemaker, A. H. de Vries, I. Faustino, Z. Meng, W. Szymanski, A. Herrmann, B. L. Feringa, *J. Am. Chem. Soc.* **2018**, *140*, 5069–5076; d) G. Ragazzon, M. Baroncini, S. Silvi, M. Venturi, A. Credi, *Nat. Nanotechnol.* **2015**, *10*, 70–75; e) M. Canton, J. Groppi, L. Casimiro, S. Corra, M. Baroncini, S. Silvi, A. Credi, *J. Am. Chem. Soc.* **2021**, *143*, 10890–10894.
- [29] a) W. Wen, W. Q. Ouyang, S. Guan, A. H. Chen, *Polym. Chem.* **2021**, *12*, 458–465; b) X. Zheng, S. Guan, C. Zhang, T. Qu, W. Wen, Y. Zhao, A. Chen, *Small* **2019**, *15*, e1900110; c) A. Natansohn, P. Rochon, *Chem. Rev.* **2002**, *102*, 4139–4175; d) J. Park, D. Yuan, K. T. Pham, J. R. Li, A. Yakovenko, H. C. Zhou, *J. Am. Chem. Soc.* **2012**, *134*, 99–102.
- [30] a) M. Dong, A. Babalhavaej, S. Samanta, A. A. Beharry, G. A. Woolley, *Acc. Chem. Res.* **2015**, *48*, 2662–2670; b) C. Poloni, W. Szymanski, L. Hou, W. R. Browne, B. L. Feringa, *Chem. Eur. J.* **2014**, *20*, 946–951; c) U. A. Hrozhyk, S. V. Serak, N. V. Tabiryan, L. Hoke, D. M. Steeves, B. Kimball, G. Kedziora, *Mol. Cryst. Liq. Cryst.* **2011**, *489*, 257/[583]–272/[598]; d) A. Goulet-Hanssens, T. C. Corkery, A. Priimagi, C. J. Barrett, *J. Mater. Chem. C* **2014**, *2*, 7505–7512.
- [31] J. Garcia-Amoros, D. Velasco, *Beilstein J. Org. Chem.* **2012**, *8*, 1003–1017.
- [32] N. A. Wazzan, P. R. Richardson, A. C. Jones, *Photochem. Photobiol. Sci.* **2010**, *9*, 968–974.
- [33] a) S. Samanta, T. M. McCormick, S. K. Schmidt, D. S. Seferos, G. A. Woolley, *Chem. Commun. (Camb.)* **2013**, *49*, 10314–10316; b) K. Kuntze, J. Viljakka, E. Titov, Z. Ahmed, E. Kalenius, P. Saalfrank, A. Priimagi, *Photochem. Photobiol. Sci.* **2021**.
- [34] O. Sadovski, A. A. Beharry, F. Zhang, G. A. Woolley, *Angew. Chem. Int. Ed. Engl.* **2009**, *48*, 1484–1486.
- [35] A. A. Beharry, O. Sadovski, G. A. Woolley, *J. Am. Chem. Soc.* **2011**, *133*, 19684–19687.
- [36] S. Samanta, A. A. Beharry, O. Sadovski, T. M. McCormick, A. Babalhavaej, V. Tropepe, G. A. Woolley, *J. Am. Chem. Soc.* **2013**, *135*, 9777–9784.
- [37] M. Wegener, M. J. Hansen, A. J. M. Driessen, W. Szymanski, B. L. Feringa, *J. Am. Chem. Soc.* **2017**, *139*, 17979–17986.
- [38] A. Rullo, A. Reiter, A. Reiter, D. Trauner, E. Y. Isacoff, G. A. Woolley, *Chem. Commun. (Camb.)* **2014**, *50*, 14613–14615.

- [39] a) D. B. Konrad, J. A. Frank, D. Trauner, *Chem. Eur. J.* **2016**, *22*, 4364–4368; b) M. J. Hansen, M. M. Lerch, W. Szymanski, B. L. Feringa, *Angew. Chem. Int. Ed. Engl.* **2016**, *55*, 13514–13518.
- [40] L. N. Lameijer, S. Budzak, N. A. Simeth, M. J. Hansen, B. L. Feringa, D. Jacquemin, W. Szymanski, *Angew. Chem. Int. Ed. Engl.* **2020**, *59*, 21663–21670.
- [41] D. Blegler, J. Schwarz, A. M. Brouwer, S. Hecht, *J. Am. Chem. Soc.* **2012**, *134*, 20597–20600.
- [42] A. L. Leistner, S. Kirchner, J. Karcher, T. Bantle, M. L. Schulte, P. Godtel, C. Fengler, Z. L. Pianowski, *Chem. Eur. J.* **2021**, *27*, 8094–8099.
- [43] D. B. Konrad, G. Savasci, L. Allmendinger, D. Trauner, C. Ochsenfeld, A. M. Ali, *J. Am. Chem. Soc.* **2020**, *142*, 6538–6547.
- [44] S. Stoyanov, L. Antonov, T. Stoyanova, V. Petrova, *Dyes Pigm.* **1996**, *32*, 171–185.
- [45] S. Samanta, A. Babalhavaeji, M. X. Dong, G. A. Woolley, *Angew. Chem. Int. Ed. Engl.* **2013**, *52*, 14127–14130.
- [46] a) R. S. L. Gibson, J. Calbo, M. J. Fuchter, *ChemPhotoChem* **2019**, *3*, 372–377; b) M. Dong, A. Babalhavaeji, M. J. Hansen, L. Kalman, G. A. Woolley, *Chem. Commun. (Camb.)* **2015**, *51*, 12981–12984; c) G. Feraud, C. Dedonder-Lardeux, C. Jouvét, E. Marceca, *J. Phys. Chem. A* **2016**, *120*, 3897–3905.
- [47] M. Dong, A. Babalhavaeji, C. V. Collins, K. Jarrah, O. Sadovski, Q. Dai, G. A. Woolley, *J. Am. Chem. Soc.* **2017**, *139*, 13483–13486.
- [48] S. Crespi, N. A. Simeth, B. Koinig, *Nat. Chem. Rev.* **2019**, *3*, 133–146.
- [49] C. E. Weston, R. D. Richardson, P. R. Haycock, A. J. White, M. J. Fuchter, *J. Am. Chem. Soc.* **2014**, *136*, 11878–11881.
- [50] N. A. Simeth, S. Crespi, M. Fagnoni, B. König, *J. Am. Chem. Soc.* **2018**, *140*, 2940–2946.
- [51] T. Wendler, C. Schutt, C. Nather, R. Herges, *J. Org. Chem.* **2012**, *77*, 3284–3287.
- [52] J. Calbo, C. E. Weston, A. J. White, H. S. Rzepa, J. Contreras-Garcia, M. J. Fuchter, *J. Am. Chem. Soc.* **2017**, *139*, 1261–1274.
- [53] A. D. W. Kennedy, I. Sandler, J. Andreasson, J. Ho, J. E. Beves, *Chem. Eur. J.* **2020**, *26*, 1103–1110.
- [54] R. Siewertsen, H. Neumann, B. Buchheim-Stehn, R. Herges, C. Nather, F. Renth, F. Temps, *J. Am. Chem. Soc.* **2009**, *131*, 15594–15595.
- [55] a) P. Lentès, E. Stadler, F. Rohricht, A. Brahms, J. Grobner, F. D. Sonnichsen, G. Geschiedt, R. Herges, *J. Am. Chem. Soc.* **2019**, *141*, 13592–13600; b) M. Hammerich, C. Schutt, C. Stahler, P. Lentès, F. Rohricht, R. Hoppner, R. Herges, *J. Am. Chem. Soc.* **2016**, *138*, 13111–13114.
- [56] P. Lentès, J. Rudtke, T. Griebenow, R. Herges, *Beilstein J. Org. Chem.* **2021**, *17*, 1503–1508.
- [57] Y. Yang, R. P. Hughes, I. Aprahamian, *J. Am. Chem. Soc.* **2012**, *134*, 15221–15224.
- [58] Y. Yang, R. P. Hughes, I. Aprahamian, *J. Am. Chem. Soc.* **2014**, *136*, 13190–13193.
- [59] H. Qian, Y. Y. Wang, D. S. Guo, I. Aprahamian, *J. Am. Chem. Soc.* **2017**, *139*, 1037–1040.
- [60] H. Qian, B. H. Shao, I. Aprahamian, *Tetrahedron* **2017**, *73*, 4901–4904.
- [61] R. Paul, R. S. Blackburn, T. Bechtold, in *Ullmann's Encyclopedia of Industrial Chemistry*, **2021**, pp. 1–16.
- [62] J. Pina, D. Sarmiento, M. Accoto, P. L. Gentili, L. Vaccaro, A. Galvao, J. S. Seixas de Melo, *J. Phys. Chem. B* **2017**, *121*, 2308–2318.
- [63] T. Arai, M. Ikegami, *Chem. Lett.* **1999**, *28*, 965–966.
- [64] M. Ikegami, T. Arai, *Bull. Chem. Soc. Jpn.* **2003**, *76*, 1783–1792.
- [65] C. Petermayer, S. Thumser, F. Kink, P. Mayer, H. Dube, *J. Am. Chem. Soc.* **2017**, *139*, 15060–15067.
- [66] a) T. Cordes, T. Schadendorf, B. Priewisch, K. Ruck-Braun, W. Zinth, *J. Phys. Chem. A* **2008**, *112*, 581–588; b) A. Nenov, T. Cordes, T. T. Herzog, W. Zinth, R. de Vivie-Riedle, *J. Phys. Chem. A* **2010**, *114*, 13016–13030.
- [67] K. Ichimura, T. Seki, T. Tamaki, T. Yamaguchi, *Chem. Lett.* **1990**, *19*, 1645–1646.
- [68] F. Kink, M. P. Collado, S. Wiedbrauk, P. Mayer, H. Dube, *Chem. Eur. J.* **2017**, *23*, 6237–6243.
- [69] J. E. Zweig, T. R. Newhouse, *J. Am. Chem. Soc.* **2017**, *139*, 10956–10959.
- [70] a) S. Wiedbrauk, B. Maerz, E. Samoylova, P. Mayer, W. Zinth, H. Dube, *J. Phys. Chem. Lett.* **2017**, *8*, 1585–1592; b) S. Wiedbrauk, B. Maerz, E. Samoylova, A. Reiner, F. Trommer, P. Mayer, W. Zinth, H. Dube, *J. Am. Chem. Soc.* **2016**, *138*, 12219–12227.
- [71] A. Gerwien, M. Schildhauer, S. Thumser, P. Mayer, H. Dube, *Nat. Commun.* **2018**, *9*, 2510.
- [72] a) M. Guentner, M. Schildhauer, S. Thumser, P. Mayer, D. Stephenson, P. J. Mayer, H. Dube, *Nat. Commun.* **2015**, *6*, 8406; b) R. Wilcken, M. Schildhauer, F. Rott, L. A. Huber, M. Guentner, S. Thumser, K. Hoffmann, S. Oesterling, R. de Vivie-Riedle, E. Riedle, H. Dube, *J. Am. Chem. Soc.* **2018**, *140*, 5311–5318; c) L. A. Huber, K. Hoffmann, S. Thumser, N. Bocher, P. Mayer, H. Dube, *Angew. Chem. Int. Ed. Engl.* **2017**, *56*, 14536–14539; d) A. Gerwien, P. Mayer, H. Dube, *J. Am. Chem. Soc.* **2018**, *140*, 16442–16445.
- [73] a) J. Weinstein, G. M. Wyman, *J. Am. Chem. Soc.* **2002**, *78*, 4007–4010; b) C. R. Giuliano, L. D. Hess, J. D. Margerum, *J. Am. Chem. Soc.* **1968**, *90*, 587–594.
- [74] C. Y. Huang, A. Bonasera, L. Hristov, Y. Garmshausen, B. M. Schmidt, D. Jacquemin, S. Hecht, *J. Am. Chem. Soc.* **2017**, *139*, 15205–15211.
- [75] M. W. H. Hoorens, M. Medved, A. D. Laurent, M. Di Donato, S. Fanetti, L. Slappendel, M. Hilbers, B. L. Feringa, W. Jan Buma, W. Szymanski, *Nat. Commun.* **2019**, *10*, 2390.
- [76] M. Medved, M. W. H. Hoorens, M. Di Donato, A. D. Laurent, J. Fan, M. Taddei, M. Hilbers, B. L. Feringa, W. J. Buma, W. Szymanski, *Chem. Sci.* **2021**, *12*, 4588–4598.
- [77] M. Irie, *Chem. Rev.* **2000**, *100*, 1685–1716.
- [78] Z. Y. Li, C. J. He, Z. Q. Lu, P. S. Li, Y. P. Zhu, *Dyes Pigm.* **2020**, *182*.
- [79] a) G. M. Tsivgoulis, J. M. Lehn, *Adv. Mater.* **1997**, *9*, 627–630; b) O. Tosic, K. Altenhoner, J. Mattay, *Photochem. Photobiol. Sci.* **2010**, *9*, 128–130; c) T. Fukaminato, T. Hirose, T. Doi, M. Hazama, K. Matsuda, M. Irie, *J. Am. Chem. Soc.* **2014**, *136*, 17145–17154.
- [80] S. L. Tang, F. L. Song, M. H. Lu, K. L. Han, X. J. Peng, *Sci. China Chem.* **2019**, *62*, 451–459.
- [81] N. M. Wu, M. Ng, W. H. Lam, H. L. Wong, V. W. Yam, *J. Am. Chem. Soc.* **2017**, *139*, 15142–15150.
- [82] C. T. Poon, W. H. Lam, H. L. Wong, V. W. Yam, *J. Am. Chem. Soc.* **2010**, *132*, 13992–13993.
- [83] Z. Li, Y. Wang, M. Li, H. Chen, Y. Xie, P. Li, H. Guo, H. Ya, *Dyes Pigm.* **2019**, *162*, 339–347.
- [84] a) R. T. Jukes, V. Adamo, F. Hartl, P. Belsler, L. De Cola, *Inorg. Chem.* **2004**, *43*, 2779–2792; b) Z. Zhang, W. Wang, P. Jin, J. Xue, L. Sun, J. Huang, J. Zhang, H. Tian, *Nat. Commun.* **2019**, *10*, 4232; c) S. Fredrich, R. Gostl, M. Herder, L. Grubert, S. Hecht, *Angew. Chem. Int. Ed. Engl.* **2016**, *55*, 1208–1212.
- [85] K. Mori, Y. Ishibashi, H. Matsuda, S. Ito, Y. Nagasawa, H. Nakagawa, K. Uchida, S. Yokojima, S. Nakamura, M. Irie, H. Miyasaka, *J. Am. Chem. Soc.* **2011**, *133*, 2621–2625.
- [86] H. Xi, Z. Zhang, W. Zhang, M. Li, C. Lian, Q. Luo, H. Tian, W. H. Zhu, *J. Am. Chem. Soc.* **2019**, *141*, 18467–18474.
- [87] J. C. Boyer, C. J. Carling, B. D. Gates, N. R. Branda, *J. Am. Chem. Soc.* **2010**, *132*, 15766–15772.
- [88] Y. Mi, H. B. Cheng, H. Chu, J. Zhao, M. Yu, Z. Gu, Y. Zhao, L. Li, *Chem. Sci.* **2019**, *10*, 10231–10239.
- [89] H. R. Blattmann, D. Meuche, E. Heilbronner, R. J. Molyneux, V. Boekelheide, *J. Am. Chem. Soc.* **2002**, *87*, 130–131.
- [90] R. H. Mitchell, Y. S. Chen, *Tetrahedron Lett.* **1996**, *37*, 5239–5242.
- [91] R. H. Mitchell, T. R. Ward, Y. Chen, Y. Wang, S. A. Weerawarna, P. W. Dibble, M. J. Marsella, A. Almutairi, Z. Q. Wang, *J. Am. Chem. Soc.* **2003**, *125*, 2974–2988.
- [92] a) R. H. Mitchell, *Eur. J. Org. Chem.* **1999**, *1999*, 2695–2703; b) R. H. Mitchell, S. Bandyopadhyay, *Org. Lett.* **2004**, *6*, 1729–1732.
- [93] K. Klauze, W. Han, P. Liesfeld, F. Berger, Y. Garmshausen, S. Hecht, *J. Am. Chem. Soc.* **2020**, *142*, 11857–11864.
- [94] K. Klauze, Y. Garmshausen, S. Hecht, *Angew. Chem. Int. Ed. Engl.* **2018**, *57*, 1414–1417.
- [95] P. Liesfeld, Y. Garmshausen, S. Budzak, J. Becker, A. Dallmann, D. Jacquemin, S. Hecht, *Angew. Chem. Int. Ed. Engl.* **2020**, *59*, 19352–19358.
- [96] D. Roldan, S. Cobo, F. Lafolet, N. Vila, C. Bochot, C. Bucher, E. Saint-Aman, M. Boggio-Pasqua, M. Garavelli, G. Royal, *Chem. Eur. J.* **2015**, *21*, 455–467.
- [97] M. Jacquet, F. Lafolet, S. Cobo, F. Loiseau, A. Bakkar, M. Boggio-Pasqua, E. Saint-Aman, G. Royal, *Inorg. Chem.* **2017**, *56*, 4357–4368.
- [98] M. Jacquet, L. M. Uriarte, F. Lafolet, M. Boggio-Pasqua, M. Sliwa, F. Loiseau, E. Saint-Aman, S. Cobo, G. Royal, *J. Phys. Chem. Lett.* **2020**, *11*, 2682–2688.
- [99] J. Hine, J. A. Brown, L. H. Zalkow, W. E. Gardner, M. Hine, *J. Am. Chem. Soc.* **2002**, *77*, 594–598.
- [100] A. F. Plate, M. A. Pryanishnikova, *Bull. Acad. Sci. USSR Div. Chem. Sci. (Engl. Transl.)* **1956**, *5*, 753–754.
- [101] A. D. Dubonosov, V. A. Bren, V. A. Chernovianov, *Russ. Chem. Rev.* **2002**, *71*, 917–927.
- [102] K. Maruyama, K. Terada, Y. Yamamoto, *Chem. Lett.* **1981**, *10*, 839–842.

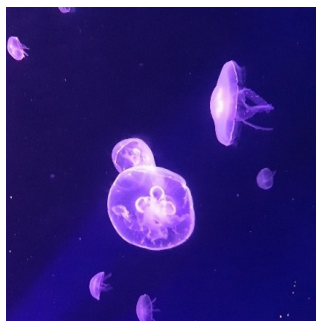
- [103] V. Gray, A. Lennartson, P. Ratanalert, K. Borjesson, K. Moth-Poulsen, *Chem. Commun. (Camb.)* **2014**, 50, 5330–5332.
- [104] M. Manso, B. E. Tebikachew, K. Moth-Poulsen, M. B. Nielsen, *Org. Biomol. Chem.* **2018**, 16, 5585–5590.
- [105] M. Manso, M. D. Kilde, S. K. Singh, P. Erhart, K. Moth-Poulsen, M. B. Nielsen, *Phys. Chem. Chem. Phys.* **2019**, 21, 3092–3097.
- [106] S. Helmy, F. A. Leibfarth, S. Oh, J. E. Poelma, C. J. Hawker, J. Read de Alaniz, *J. Am. Chem. Soc.* **2014**, 136, 8169–8172.
- [107] a) M. M. Lerch, S. J. Wezenberg, W. Szymanski, B. L. Feringa, *J. Am. Chem. Soc.* **2016**, 138, 6344–6347; b) M. M. Lerch, W. Szymanski, B. L. Feringa, *Chem. Soc. Rev.* **2018**, 47, 1910–1937.
- [108] S. O. Poelma, S. S. Oh, S. Helmy, A. S. Knight, G. L. Burnett, H. T. Soh, C. J. Hawker, J. Read de Alaniz, *Chem. Commun. (Camb.)* **2016**, 52, 10525–10528.
- [109] a) J. R. Hemmer, S. O. Poelma, N. Treat, Z. A. Page, N. D. Dolinski, Y. J. Diaz, W. Tomlinson, K. D. Clark, J. P. Hooper, C. Hawker, J. Read de Alaniz, *J. Am. Chem. Soc.* **2016**, 138, 13960–13966; b) N. Mallo, P. T. Brown, H. Iranmanesh, T. S. MacDonald, M. J. Teusner, J. B. Harper, G. E. Ball, J. E. Beves, *Chem. Commun. (Camb.)* **2016**, 52, 13576–13579.
- [110] J. R. Hemmer, Z. A. Page, K. D. Clark, F. Stricker, N. D. Dolinski, C. J. Hawker, J. Read de Alaniz, *J. Am. Chem. Soc.* **2018**, 140, 10425–10429.
- [111] M. M. Lerch, M. Di Donato, A. D. Laurent, M. Medved, A. Iagatti, L. Bussotti, A. Lapini, W. J. Buma, P. Foggi, W. Szymanski, B. L. Feringa, *Angew. Chem. Int. Ed. Engl.* **2018**, 57, 8063–8068.
- [112] S. W. Connolly, R. Tiwari, S. J. Holder, H. J. Shepherd, *Phys. Chem. Chem. Phys.* **2021**, 23, 2775–2779.
- [113] a) B. H. Shao, I. Aprahamian, *Chem* **2020**, 6, 2162–2173; b) I. Aprahamian, *Chem. Commun. (Camb.)* **2017**, 53, 6674–6684.
- [114] a) R. Pichon, J. Le Saint, P. Courtot, *Tetrahedron* **1981**, 37, 1517–1524; b) M. N. Chaur, D. Collado, J. M. Lehn, *Chem. Eur. J.* **2011**, 17, 248–258.
- [115] H. Qian, S. Pramanik, I. Aprahamian, *J. Am. Chem. Soc.* **2017**, 139, 9140–9143.
- [116] B. Shao, H. Qian, Q. Li, I. Aprahamian, *J. Am. Chem. Soc.* **2019**, 141, 8364–8371.
- [117] J. H. Day, *Chem. Rev.* **1963**, 63, 65–80.
- [118] Y. Hirshberg, E. Fischer, *J. Chem. Soc.* **1954**, 297–303.
- [119] L. Kortekaas, J. Chen, D. Jacquemin, W. R. Browne, *J. Phys. Chem. B* **2018**, 122, 6423–6430.
- [120] J. Buback, M. Kullmann, F. Langhojer, P. Nuernberger, R. Schmidt, F. Wurthner, T. Brixner, *J. Am. Chem. Soc.* **2010**, 132, 16510–16519.
- [121] D. A. Parthenopoulos, P. M. Rentzepis, *Science* **1989**, 245, 843–845.
- [122] O. Ivashenko, J. T. van Herpt, B. L. Feringa, P. Rudolf, W. R. Browne, *J. Phys. Chem. C* **2013**, 117, 18567–18577.
- [123] T. Stafforst, D. Hilvert, *Chem. Commun. (Camb.)* **2009**, 287–288.
- [124] Y. Zhang, S. Tang, E. R. Thapaliya, L. Sansalone, F. M. Raymo, *Chem. Commun. (Camb.)* **2018**, 54, 8799–8809.
- [125] R. Klajn, *Chem. Soc. Rev.* **2014**, 43, 148–184.
- [126] F. D. Jochum, P. Theato, *Chem. Soc. Rev.* **2013**, 42, 7468–7483.
- [127] K. Kumar, C. Knie, D. Bleger, M. A. Peletier, H. Friedrich, S. Hecht, D. J. Broer, M. G. Debije, A. P. Schenning, *Nat. Commun.* **2016**, 7, 11975.
- [128] A. H. Gelebart, D. J. Mulder, G. Vantomme, A. Schenning, D. J. Broer, *Angew. Chem. Int. Ed. Engl.* **2017**, 56, 13436–13439.
- [129] H. Zeng, O. M. Wani, P. Wasylczyk, A. Priimagi, *Macromol. Rapid Commun.* **2018**, 39, 1700224.
- [130] G. Vantomme, A. H. Gelebart, D. J. Broer, E. W. Meijer, *Tetrahedron* **2017**, 73, 4963–4967.
- [131] A. Ryabchun, Q. Li, F. Lancia, I. Aprahamian, N. Katsonis, *J. Am. Chem. Soc.* **2019**, 141, 1196–1200.
- [132] J. Lee, M. M. Sroda, Y. Kwon, S. El-Arid, S. Seshadri, L. F. Gockowski, E. W. Hawkes, M. T. Valentine, J. Read de Alaniz, *ACS Appl. Mater. Interfaces* **2020**, 12, 54075–54082.
- [133] S. H. Mostafavi, W. Li, K. D. Clark, F. Stricker, J. R. d. Alaniz, C. J. Bardeen, *Macromolecules* **2019**, 52, 6311–6317.
- [134] S. H. Mostafavi, F. Tong, T. W. Dugger, D. Kisailus, C. J. Bardeen, *Macromolecules* **2018**, 51, 2388–2394.
- [135] B. F. Lui, N. T. Tierce, F. Tong, M. M. Sroda, H. Lu, J. Read de Alaniz, C. J. Bardeen, *Photochem. Photobiol. Sci.* **2019**, 18, 1587–1595.
- [136] A. Balamurugan, H.-i. Lee, *Macromolecules* **2016**, 49, 2568–2574.
- [137] D. Zhong, Z. Q. Cao, B. Wu, Q. Zhang, G. J. Wang, *Sens. Actuators B* **2018**, 254, 385–392.
- [138] B. Zuo, M. Wang, B. P. Lin, H. Yang, *Chem. Mater.* **2018**, 30, 8079–8088.
- [139] S. Ghosh, M. S. Hossain, S. Chatterjee, S. A. Rahaman, S. Bandyopadhyay, *ACS Appl. Mater. Interfaces* **2020**, 12, 52983–52991.
- [140] D. Wang, M. Wagner, H. J. Butt, S. Wu, *Soft Matter* **2015**, 11, 7656–7662.
- [141] J. Karcher, Z. L. Pianowski, *Chem. Eur. J.* **2018**, 24, 11605–11610.
- [142] J. Karcher, S. Kirchner, A. L. Leistner, C. Hald, P. Geng, T. Bantle, P. Godtel, J. Pfeifer, Z. L. Pianowski, *RSC Adv.* **2021**, 11, 8546–8551.
- [143] F. Zhao, A. Bonasera, U. Nochel, M. Behl, D. Bleger, *Macromol. Rapid Commun.* **2018**, 39, 1700527.
- [144] X. Tong, Y. Qiu, X. Zhao, B. Xiong, R. Liao, H. Peng, Y. Liao, X. Xie, *Soft Matter* **2019**, 15, 6411–6417.
- [145] Y. Wang, M. Li, C. Yan, N. Ma, Y. Chen, *CCS* **2022**, 4, 704–712.
- [146] Z. I. Yoshida, *J. Photochem.* **1985**, 29, 27–40.
- [147] Z. Wang, J. Udmark, K. Borjesson, R. Rodrigues, A. Roffey, M. Abrahamsson, M. B. Nielsen, K. Moth-Poulsen, *ChemSusChem* **2017**, 10, 3049–3055.
- [148] M. Manso, L. Fernandez, Z. Wang, K. Moth-Poulsen, M. B. Nielsen, *Molecules* **2020**, 25.
- [149] J. Orrego-Hernandez, A. Dreos, K. Moth-Poulsen, *Acc. Chem. Res.* **2020**, 53, 1478–1487.
- [150] A. U. Petersen, A. I. Hofmann, M. Fillols, M. Manso, M. Jevric, Z. Wang, C. J. Sumbly, C. Muller, K. Moth-Poulsen, *Adv. Sci.* **2019**, 6, 1900367.
- [151] A. Dreos, K. Borjesson, Z. H. Wang, A. Roffey, Z. Norwood, D. Kushnir, K. Moth-Poulsen, *Energy Environ. Sci.* **2017**, 10, 728–734.
- [152] Y. R. Shi, M. A. Gerkman, Q. F. Qiu, S. R. Zhang, G. G. D. Han, *J. Mater. Chem. A* **2021**, 9, 9798–9808.
- [153] L. S. Xie, G. Skorupskii, M. Dinca, *Chem. Rev.* **2020**, 120, 8536–8580.
- [154] X. Fang, B. Zong, S. Mao, *Nano-Micro Lett.* **2018**, 10, 64.
- [155] D. W. Lim, J. S. Ha, Y. Oruganti, H. R. Moon, *Mater. Chem. Front.* **2021**, 5, 4022–4041.
- [156] X. Ma, M. Lepoitevin, C. Serre, *Mater. Chem. Front.* **2021**, 5, 5573–5594.
- [157] B. N. Zheng, X. D. Lin, X. C. Zhang, D. C. Wu, K. Matyjaszewski, *Adv. Funct. Mater.* **2020**, 30.
- [158] a) N. K. Kulachenkov, D. Sun, Y. A. Mezenov, A. N. Yankin, S. Rzhetskiy, V. Dyachuk, A. Nomine, G. Medjahdi, E. A. Pidko, V. A. Milichko, *Angew. Chem. Int. Ed. Engl.* **2020**, 59, 15522–15526; b) S. Castellanos, A. Goulet-Hanssens, F. Zhao, A. Dikhtiarenko, A. Pustovarenko, S. Hecht, J. Gascon, F. Kapteijn, D. Bleger, *Chem. Eur. J.* **2016**, 22, 746–752; c) D. Mutruc, A. Goulet-Hanssens, S. Fairman, S. Wahl, A. Zimathies, C. Knie, S. Hecht, *Angew. Chem. Int. Ed. Engl.* **2019**, 58, 12862–12867; d) L. Pesce, C. Perego, A. B. Grommet, R. Klajn, G. M. Pavan, *J. Am. Chem. Soc.* **2020**, 142, 9792–9802; e) A. I. Hanopolskiy, S. De, M. J. Bialek, Y. Diskin-Posner, L. Avram, M. Feller, R. Klajn, *Beilstein J. Org. Chem.* **2019**, 15, 2398–2407; f) M. Canton, A. B. Grommet, L. Pesce, J. Gemen, S. Li, Y. Diskin-Posner, A. Credi, G. M. Pavan, J. Andreasson, R. Klajn, *J. Am. Chem. Soc.* **2020**, 142, 14557–14565.
- [159] Y. Zheng, H. Sato, P. Wu, H. J. Jeon, R. Matsuda, S. Kitagawa, *Nat. Commun.* **2017**, 8, 100.
- [160] Z. Wang, A. Knebel, S. Grosjean, D. Wagner, S. Brase, C. Woll, J. Caro, L. Heinke, *Nat. Commun.* **2016**, 7, 13872.
- [161] Y. Jiang, L. Heinke, *Langmuir* **2021**, 37, 2–15.
- [162] K. Muller, A. Knebel, F. Zhao, D. Bleger, J. Caro, L. Heinke, *Chem. Eur. J.* **2017**, 23, 5434–5438.
- [163] H.-Q. Liang, Y. Guo, X. Peng, B. Chen, *J. Mater. Chem. A* **2020**, 8, 11399–11405.
- [164] D. Samanta, D. Galaktionova, J. Gemen, L. J. W. Shimon, Y. Diskin-Posner, L. Avram, P. Kral, R. Klajn, *Nat. Commun.* **2018**, 9, 641.
- [165] D. Samanta, J. Gemen, Z. Chu, Y. Diskin-Posner, L. J. W. Shimon, R. Klajn, *Proc. Natl. Acad. Sci. USA* **2018**, 115, 9379–9384.
- [166] H. Chen, N. Cheng, W. Ma, M. Li, S. Hu, L. Gu, S. Meng, X. Guo, *ACS Nano* **2016**, 10, 436–445.
- [167] S. Kumar, M. Merelli, W. Danowski, P. Rudolf, B. L. Feringa, R. C. Chiechi, *Adv. Mater.* **2019**, 31, e1807831.
- [168] G. Ligorio, G. F. Cotella, A. Bonasera, N. Zorn Morales, G. Carnicella, B. Kobin, Q. Wang, N. Koch, S. Hecht, E. J. W. List-Kratochvil, F. Cacialli, *Nanoscale* **2020**, 12, 5444–5451.
- [169] a) E. Benassi, S. Corni, *J. Phys. Chem. C* **2014**, 118, 25906–25917; b) C. Gahl, R. Schmidt, D. Brete, S. Paarmann, M. Weinelt, *Surf. Sci.* **2016**, 643, 183–189.
- [170] R. Klajn, *Pure Appl. Chem.* **2010**, 82, 2247–2279.
- [171] S. Singh, K. Friedel, M. Himmerlich, Y. Lei, G. Schlingloff, A. Schober, *ACS Macro Lett.* **2015**, 4, 1273–1277.
- [172] J. Ahrens, T. Bian, T. Vexler, R. Klajn, *ChemPhotoChem* **2017**, 1, 230–236.
- [173] G. Sobczak, I. Misztalewska-Turkiewicz, V. Sashuk, *J. Phys. Chem. C* **2021**, 125, 5306–5314.
- [174] J. Kubitschke, C. Nather, R. Herges, *Eur. J. Org. Chem.* **2010**, 2010, 5041–5055.
- [175] R. Low, T. Rusch, T. Moje, F. Rohricht, O. M. Magnussen, R. Herges, *Beilstein J. Org. Chem.* **2019**, 15, 1815–1821.
- [176] M. Hammerich, R. Herges, *J. Org. Chem.* **2015**, 80, 11233–11236.

- [177] R. Low, T. Rusch, F. Rohricht, O. Magnussen, R. Herges, *Beilstein J. Org. Chem.* **2019**, *15*, 1485–1490.
- [178] S. Hagen, P. Kate, M. V. Peters, S. Hecht, M. Wolf, P. Tegeder, *Appl. Phys. A* **2008**, *93*, 253–260.
- [179] N. Moller, T. Hellwig, L. Stricker, S. Engel, C. Fallnich, B. J. Ravoo, *Chem. Commun. (Camb.)* **2016**, *53*, 240–243.
- [180] Q. Wang, G. Ligorio, R. Schlesinger, V. Diez-Cabanes, D. Cornil, Y. Garmshausen, S. Hecht, J. Cornil, E. J. W. List-Kratochvil, N. Koch, *Adv. Mater. Interfaces* **2019**, *6*.
- [181] C. Zhou, H. Zhang, Z. Li, W. Wang, *Lab Chip* **2016**, *16*, 1797–1811.
- [182] S. Seshadri, L. F. Gockowski, J. Lee, M. Sroda, M. E. Helgeson, J. Read de Alaniz, M. T. Valentine, *Nat. Commun.* **2020**, *11*, 2599.
- [183] H. Wang, H. K. Bisoyi, B. X. Li, M. E. McConney, T. J. Bunning, Q. Li, *Angew. Chem. Int. Ed. Engl.* **2020**, *59*, 2684–2687.
- [184] S. Jia, J. D. Du, A. Hawley, W. K. Fong, B. Graham, B. J. Boyd, *Langmuir* **2017**, *33*, 2215–2221.
- [185] S. Jia, A. Tan, A. Hawley, B. Graham, B. J. Boyd, *J. Colloid Interface Sci.* **2019**, *548*, 151–159.
- [186] a) S. Pujals, N. Feiner-Gracia, P. Delcanale, I. Voets, L. Albertazzi, *Nat. Chem. Rev.* **2019**, *3*, 68–84; b) O. Nevskiy, D. Sysoiev, J. Dreier, S. C. Stein, A. Oppermann, F. Lemken, T. Janke, J. Enderlein, I. Testa, T. Huhn, D. Woll, *Small* **2018**, *14*, 1703333.
- [187] S. J. Sahl, S. W. Hell, S. Jakobs, *Nat. Rev. Mol. Cell Biol.* **2017**, *18*, 685–701.
- [188] E. Kozma, P. Kele, *Org. Biomol. Chem.* **2019**, *17*, 215–233.
- [189] a) B. Roubinet, M. L. Bossi, P. Alt, M. Leutenegger, H. Shojaei, S. Schnorrenberg, S. Nizamov, M. Irie, V. N. Belov, S. W. Hell, *Angew. Chem. Int. Ed. Engl.* **2016**, *55*, 15429–15433; b) K. Uno, M. L. Bossi, T. Konen, V. N. Belov, M. Irie, S. W. Hell, *Adv. Opt. Mater.* **2019**, *7*, 1801746.
- [190] a) A. T. Frawley, V. Wycisk, Y. Xiong, S. Galiani, E. Sezgin, I. Urbancic, A. Vargas Jentzsch, K. G. Leslie, C. Eggeling, H. L. Anderson, *Chem. Sci.* **2020**, *11*, 8955–8960; b) Z. Z. Li, L. L. Liu, Y. F. Liu, *New J. Chem.* **2021**, *45*, 9872–9881.
- [191] a) C. Li, K. Xiong, Y. Chen, C. Fan, Y. L. Wang, H. Ye, M. Q. Zhu, *ACS Appl. Mater. Interfaces* **2020**, *12*, 27651–27662; b) J. Li, R. Wang, Y. Sun, P. Xiao, S. Yang, X. Wang, Q. Fan, W. Wu, X. Jiang, *ACS Appl. Mater. Interfaces* **2021**, *13*, 54830–54839.
- [192] Y. Jing, C. Zhang, B. Yu, D. Lin, J. Qu, *Front. Chem.* **2021**, *9*, 746900.
- [193] a) J. Joshi, M. Rubart, W. Zhu, *Front. bioeng. biotechnol.* **2019**, *7*, 466; b) C. Lee, A. Lavoie, J. Liu, S. X. Chen, B. H. Liu, *Front. Neural Circuits* **2020**, *14*, 18; c) F. Kawano, H. Suzuki, A. Furuya, M. Sato, *Nat. Commun.* **2015**, *6*, 6256.
- [194] T. Fehrentz, M. Schonberger, D. Trauner, *Angew. Chem. Int. Ed. Engl.* **2011**, *50*, 12156–12182.
- [195] I. Tochitsky, M. A. Kienzler, E. Isacoff, R. H. Kramer, *Chem. Rev.* **2018**, *118*, 10748–10773.
- [196] a) M. A. Kienzler, A. Reiner, E. Trautman, S. Yoo, D. Trauner, E. Y. Isacoff, *J. Am. Chem. Soc.* **2013**, *135*, 17683–17686; b) G. Cabre, A. Garrido-Charles, A. Gonzalez-Lafont, W. Moormann, D. Langbehn, D. Egea, J. M. Lluch, R. Herges, R. Alibes, F. Busque, P. Gorostiza, J. Hernando, *Org. Lett.* **2019**, *21*, 3780–3784.
- [197] a) E. C. Carroll, S. Berlin, J. Levitz, M. A. Kienzler, Z. Yuan, D. Madsen, D. S. Larsen, E. Y. Isacoff, *Proc. Natl. Acad. Sci. USA* **2015**, *112*, E776–785; b) S. Kellner, S. Berlin, *Appl. Sci.* **2020**, *10*; c) I. Carmi, M. De Battista, L. Maddalena, E. C. Carroll, M. A. Kienzler, S. Berlin, *Nat. Protoc.* **2019**, *14*, 864–900.
- [198] X. Just-Baringo, A. Yeste-Vazquez, J. Moreno-Morales, C. Balleste-Delpierre, J. Vila, E. Giralt, *Chem. Eur. J.* **2021**, *27*, 12987–12991.
- [199] L. Zhang, G. Linden, O. Vazquez, *Beilstein J. Org. Chem.* **2019**, *15*, 2500–2508.
- [200] a) A. A. John, C. P. Ramil, Y. Tian, G. Cheng, Q. Lin, *Org. Lett.* **2015**, *17*, 6258–6261; b) C. Hoppmann, I. Maslennikov, S. Choe, L. Wang, *J. Am. Chem. Soc.* **2015**, *137*, 11218–11221; c) J. Luo, S. Samanta, M. Convertino, N. V. Dokholyan, A. Deiters, *ChemBioChem* **2018**, *19*, 2178–2185.
- [201] a) Y. Kamiya, Y. Arimura, H. Ooi, K. Kato, X. G. Liang, H. Asanuma, *ChemBioChem* **2018**, *19*, 1305–1311; b) Y. Kamiya, T. Takagi, H. Ooi, H. Ito, X. Liang, H. Asanuma, *ACS Synth. Biol.* **2015**, *4*, 365–370; c) M. L. Hammill, G. Islam, J. P. Desaulniers, *ChemBioChem* **2020**, *21*, 2367–2372.
- [202] V. Poonthiyil, F. Reise, G. Despras, T. K. Lindhorst, *Eur. J. Org. Chem.* **2018**, *2018*, 6241–6248.
- [203] S. D. Pritzl, D. B. Konrad, M. F. Ober, A. F. Richter, J. A. Frank, B. Nickel, D. Trauner, T. Lohmuller, *Langmuir* **2022**, *38*, 385–393.

Manuscript received: October 15, 2021
Revised manuscript received: February 24, 2022
Accepted manuscript online: February 25, 2022

REVIEW

In this Review, various classes of molecular photoswitches triggered with visible light are reported together with their applications in phototriggered smart materials – polymers, hydrogels, surfaces, porous materials, and sunlight energy storage materials. Advantages of such systems over classical UV-light triggered photochromic materials, the scope of their applicability, and their limitations are discussed.



*A.-L. Leistner, Dr. Z. L. Pianowski**

1 – 21

**Smart Photochromic Materials
Triggered with Visible Light**
